

Primary and Secondary Phosphine Complexes of Iron Porphyrins and Ruthenium Phthalocyanine: Synthesis, Structure, and P–H Bond Functionalization

Jie-Sheng Huang,* Guang-Ao Yu, Jin Xie, Kwok-Ming Wong, Nianyong Zhu, and Chi-Ming Che*

Department of Chemistry and Open Laboratory of Chemical Biology of the Institute of Molecular Technology for Drug Discovery and Synthesis, The University of Hong Kong, Pokfulam Road, Hong Kong

Received March 17, 2008

Reduction of $[\text{Fe}^{\text{II}}(\text{Por})\text{Cl}]$ (Por = porphyrinato dianion) with $\text{Na}_2\text{S}_2\text{O}_4$ followed by reaction with excess PH_2Ph , PH_2Ad , or PPhPh_2 afforded $[\text{Fe}^{\text{II}}(\text{F}_{20}\text{-TPP})(\text{PH}_2\text{Ph})_2]$ (**1a**), $[\text{Fe}^{\text{II}}(\text{F}_{20}\text{-TPP})(\text{PH}_2\text{Ad})_2]$ (**1b**), $[\text{Fe}^{\text{II}}(\text{F}_{20}\text{-TPP})(\text{PPhPh}_2)_2]$ (**2a**), and $[\text{Fe}^{\text{II}}(2,6\text{-Cl}_2\text{TPP})(\text{PPhPh}_2)_2]$ (**2b**). Reaction of $[\text{Ru}^{\text{II}}(\text{Pc})(\text{DMSO})_2]$ (Pc = phthalocyaninato dianion) with PH_2Ph or PPhPh_2 gave $[\text{Ru}^{\text{II}}(\text{Pc})(\text{PH}_2\text{Ph})_2]$ (**3a**) and $[\text{Ru}^{\text{II}}(\text{Pc})(\text{PPhPh}_2)_2]$ (**4**). $[\text{Ru}^{\text{II}}(\text{Pc})(\text{PH}_2\text{Ad})_2]$ (**3b**) and $[\text{Ru}^{\text{II}}(\text{Pc})(\text{PH}_2\text{Bu}^t)_2]$ (**3c**) were isolated by treating a mixture of $[\text{Ru}^{\text{II}}(\text{Pc})(\text{DMSO})_2]$ and $\text{O}=\text{PCl}_2\text{Ad}$ or PCl_2Bu^t with LiAlH_4 . Hydrophosphination of $\text{CH}_2=\text{CHR}$ (R = CO_2Et , CN) with $[\text{Ru}^{\text{II}}(\text{F}_{20}\text{-TPP})(\text{PH}_2\text{Ph})_2]$ or $[\text{Ru}^{\text{II}}(\text{F}_{20}\text{-TPP})(\text{PPhPh}_2)_2]$ in the presence of $^t\text{BuOK}$ led to the isolation of $[\text{Ru}^{\text{II}}(\text{F}_{20}\text{-TPP})(\text{P}(\text{CH}_2\text{CH}_2\text{R})_2\text{Ph}_2)]$ (R = CO_2Et , **5a**; CN, **5b**) and $[\text{Ru}^{\text{II}}(\text{F}_{20}\text{-TPP})(\text{P}(\text{CH}_2\text{CH}_2\text{R})\text{Ph}_2)_2]$ (R = CO_2Et , **6a**; CN, **6b**). Similar reaction of **3a** with $\text{CH}_2=\text{CHCN}$ or MeI gave $[\text{Ru}^{\text{II}}(\text{Pc})(\text{P}(\text{CH}_2\text{CH}_2\text{CN})_2\text{Ph}_2)]$ (**7**) or $[\text{Ru}^{\text{II}}(\text{Pc})(\text{PMe}_2\text{Ph})_2]$ (**8**). The reactions of **4** with $\text{CH}_2=\text{CHR}$ (R = CO_2Et , CN, $\text{C}(\text{O})\text{Me}$, $\text{P}(\text{O})(\text{OEt})_2$, $\text{S}(\text{O})_2\text{Ph}$), $\text{CH}_2=\text{C}(\text{Me})\text{CO}_2\text{Me}$, $\text{CH}(\text{CO}_2\text{Me})=\text{CHCO}_2\text{Me}$, MeI , BnCl , and RBr (R = ^nBu , $\text{CH}_2=\text{CHCH}_2$, $\text{MeC}\equiv\text{CCH}_2$, $\text{HC}\equiv\text{CCH}_2$) in the presence of $^t\text{BuOK}$ afforded $[\text{Ru}^{\text{II}}(\text{Pc})(\text{P}(\text{CH}_2\text{CH}_2\text{R})\text{Ph}_2)_2]$ (R = CO_2Et , **9a**; CN, **9b**; $\text{C}(\text{O})\text{Me}$, **9c**; $\text{P}(\text{O})(\text{OEt})_2$, **9d**; $\text{S}(\text{O})_2\text{Ph}$, **9e**), $[\text{Ru}^{\text{II}}(\text{Pc})(\text{P}(\text{CH}_2\text{CH}(\text{Me})\text{CO}_2\text{Me})\text{Ph}_2)_2]$ (**9f**), $[\text{Ru}^{\text{II}}(\text{Pc})(\text{P}(\text{CH}(\text{CO}_2\text{Me})\text{CH}_2\text{CO}_2\text{Me})\text{Ph}_2)_2]$ (**9g**), and $[\text{Ru}^{\text{II}}(\text{Pc})(\text{PRPh}_2)_2]$ (R = Me, **10a**; Bu^n , **10b**; Bn, **10c**; $\text{CH}_2\text{CH}=\text{CH}_2$, **10d**; $\text{CH}_2\text{C}\equiv\text{CMe}$, **10e**; $\text{CH}=\text{C}=\text{CH}_2$, **10f**). X-ray crystal structure determinations revealed Fe–P distances of 2.2597(9) (**1a**) and 2.309(2) Å (**2b** · $2\text{CH}_2\text{Cl}_2$) and Ru–P distances of 2.3707(13) (**3b**), 2.373(2) (**3c**), 2.3478(11) (**4**), and 2.3754(10) Å (**5b** · $2\text{CH}_2\text{Cl}_2$). Both the crystal structures of **3b** and **4** feature intermolecular C–H ··· π interactions, which link the molecules into 3D and 2D networks, respectively.

Introduction

Phosphines have long been used as axial ligands in the development of metalloporphyrin chemistry¹ and continue to receive considerable attention,^{2–5} including the use of phosphine complexes of iron porphyrins as models of

hemoproteins,² the employment of phosphines to stabilize rhodium complexes in low oxidation states,³ and the design of multiporphyrinic arrays based on the coordination of phosphines to metalloporphyrins.⁵ Conventionally, tertiary phosphine ligands are employed in the chemistry of metalloporphyrin complexes. Only until recently has the binding behavior of primary and secondary phosphines (PH_2R and PHR_2) to metalloporphyrins been reported in the literature; the earliest example is a work by Sanders and co-workers,⁶ reporting the in situ formation of $[\text{Ru}^{\text{II}}(\text{Por})(\text{CO})(\text{PH}_2\text{-}(\text{C}\equiv\text{CPh}))]$ and $[\text{Ru}^{\text{II}}(\text{Por})(\text{PH}_2(\text{C}\equiv\text{CPh}))_2]$, together with the

* Authors to whom correspondence should be addressed. E-mail: jshuang@hkucc.hku.hk (J.-S.H.); cmche@hku.hk (C.-M.C.).

(1) For reviews, see: (a) Buchler, J. W. In *Porphyrins and Metalloporphyrins*; Smith, K. M., Ed.; Elsevier: Amsterdam, 1975; p 157. (b) Buchler, J. W. In *The Porphyrins*; Dolphin, D., Ed.; Academic: New York, 1978; Vol. 1, p 389. (c) Mashiko, T.; Dolphin, D. In *Comprehensive Coordination Chemistry*; Wilkinson, G., Gillard, R. D., McCleverty, J. A., Eds.; Pergamon: Oxford, U.K., 1987; Vol. 2, p 813. (d) Buchler, J. W.; Dreher, C.; Kunzel, F. M. *Struct. Bonding (Berlin)* **1995**, *84*, 1. (e) Sanders, J. K. M.; Bampos, N.; Clyde-Watson, Z.; Darling, S. L.; Hawley, J. C.; Kim, H.-J.; Mak, C. C.; Webb, S. J. In *The Porphyrin Handbook*; Kadish, K. M., Smith, K. M., Guilard, R., Eds.; Academic Press: San Diego, CA, 2000; Vol. 3, p 1.

(2) (a) Simonneaux, G. *Coord. Chem. Rev.* **1997**, *165*, 447. (b) Simonneaux, G.; Bondon, A. In *The Porphyrin Handbook*; Kadish, K. M., Smith, K. M., Guilard, R., Eds.; Academic Press: San Diego, CA, 2000; Vol. 5, p 299.

(3) Collman, J. P.; Boulatov, R. *J. Am. Chem. Soc.* **2000**, *122*, 11812.

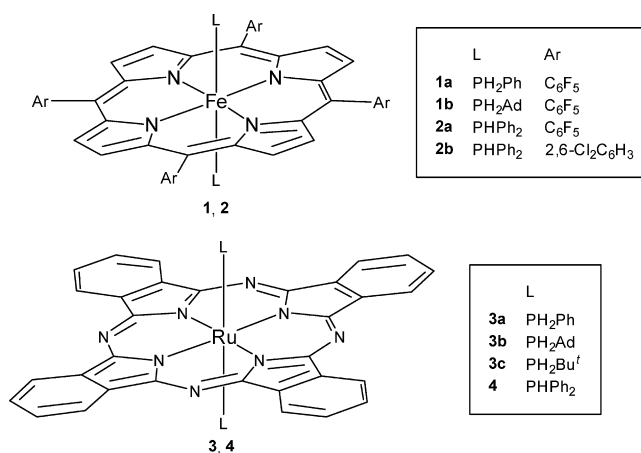
binding of a $\text{H}_2\text{P}-\text{C}\equiv\text{C}-$ or $\text{H}_2\text{P}-\text{C}=\text{C}-$ group of a nickel(II)- or zinc(II)-bound porphyrin ligand, respectively, to ruthenium and rhodium porphyrins. These primary alkynyl or alkenyl phosphine complexes are unstable in solution and have not been isolated.⁶ We have recently prepared a number of ruthenium porphyrin complexes of PH_2R (R = aryl or alkyl) and $\text{P}(\text{HPh})_2$,⁷ most of these complexes can be isolated in pure form.

Metalloporphyrins such as $[\text{M}(\text{Por})(\text{PH}_2\text{R})_2]$ and $[\text{M}(\text{Por})(\text{PHR}_2)_2]$ could be useful precursors to (i) phosphido and phosphinidene complexes of metalloporphyrins (by deprotonation), the phosphinidene complexes possibly undergoing phosphinidene transfer to alkenes or C–H bonds, analogous to the carbene or imido transfer reactions of carbene⁸ and imido metalloporphyrins,⁹ or (ii) metalloporphyrin complexes bearing various tertiary phosphine ligands (by P–H bond functionalization, which would be important either for introducing functional groups to tertiary phosphine complexes of metalloporphyrins or for tuning the electronic/steric properties of these metal complexes). Furthermore, $[\text{M}(\text{Por})(\text{PH}_2\text{R})_2]$ and $[\text{M}(\text{Por})(\text{PHR}_2)_2]$ could be considered as a unique type of the stabilized form of unstable PH_2R or PHR_2 , which have an intense unpleasant odor and are usually found to be air-sensitive. Notable recent examples are $[\text{Ru}^{\text{II}}(\text{F}_{20}\text{-TPP})(\text{PH}_2\text{Ph})_2]$ ($\text{F}_{20}\text{-TPP}$ = 5,10,15,20-tetrakis(pentafluorophenyl)porphyrinato dianion) and $[\text{Ru}^{\text{II}}(\text{F}_{20}\text{-TPP})(\text{P}(\text{HPh})_2)_2]$, both exhibiting a remarkable stability in solutions open to the air.^{7a} Being located in close proximity to porphyrin macrocycles, the coordinated P–H bonds could be functionalized with a shape- or regioselectivity. A question is whether the stabilized PH_2R and PHR_2 are active toward P–H bond functionalization reactions.

We are interested in extending the chemistry of PH_2R and PHR_2 complexes to iron porphyrins and to metallophthalocyanines. Given the presence of iron porphyrin units in hemoproteins, the binding behavior of PH_2R or PHR_2 toward iron porphyrins would provide insight into the interaction of hemoproteins with these types of phosphine substrates. Metallophthalocyanines constitute a large family of metal complexes that bear a close relationship with metallopor-

phyrins, both of which contain a large, planar macrocyclic π -conjugated ligand system. In contrast to the case of metalloporphyrins, phosphine complexes of metallophthalocyanines are less developed.¹⁰

Herein, we report the isolation of iron(II) porphyrins $[\text{Fe}^{\text{II}}(\text{Por})(\text{PH}_2\text{R})_2]$ (**1**, R = Ph, Ad (adamantyl)) and $[\text{Fe}^{\text{II}}(\text{Por})(\text{P}(\text{HPh})_2)_2]$ (**2**) and ruthenium(II) phthalocyanines $[\text{Ru}^{\text{II}}(\text{Pc})(\text{PH}_2\text{R})_2]$ (**3**, R = Ph, Ad, Bu') and $[\text{Ru}^{\text{II}}(\text{Pc})(\text{P}(\text{HPh})_2)_2]$ (**4**). The functionalization of P–H bonds in these ruthenium phthalocyanines and previously reported ruthenium porphyrin analogues has been investigated, revealing that $[\text{Ru}^{\text{II}}(\text{F}_{20}\text{-TPP})(\text{PH}_2\text{Ph})_2]$, $[\text{Ru}^{\text{II}}(\text{F}_{20}\text{-TPP})(\text{P}(\text{HPh})_2)_2]$, and their phthalocyanine counterparts can undergo hydrophosphination reactions with alkenes and P-alkylation reactions with haloalkanes. This, to the best of our knowledge, contributes the first P–H bond functionalization of primary or secondary phosphines coordinated to a metalloporphyrin and a metallophthalocyanine.



Results and Discussion

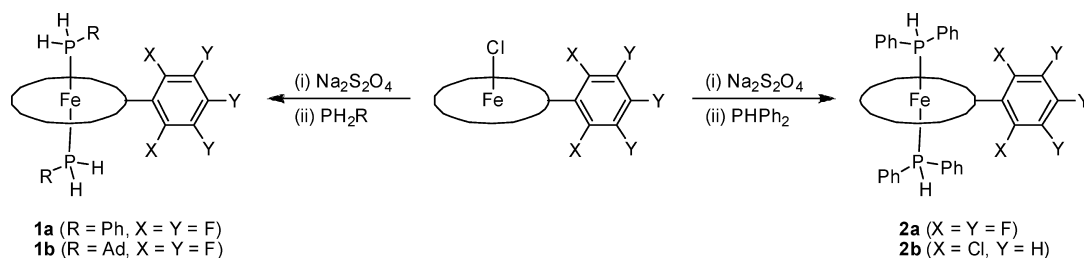
Synthesis. Reduction of $[\text{Fe}^{\text{III}}(\text{Por})\text{Cl}]$ with $\text{Na}_2\text{S}_2\text{O}_4$ followed by treatment of the in situ formed iron(II) porphyrin with excess PH_2R or $\text{P}(\text{HPh})_2$ afforded $[\text{Fe}^{\text{II}}(\text{F}_{20}\text{-TPP})(\text{PH}_2\text{R})_2]$ (R = Ph, **1a**; Ad, **1b**) or $[\text{Fe}^{\text{II}}(\text{Por})(\text{P}(\text{HPh})_2)_2]$ (Por = $\text{F}_{20}\text{-TPP}$, **2a**; 2,6- Cl_2TPP , **2b**) (2,6- Cl_2TPP = 5,10,15,20-tetrakis(2,6-dichlorophenyl)porphyrinato dianion) in about 60% yields (Scheme 1).

The phthalocyanine complexes $[\text{Ru}^{\text{II}}(\text{Pc})(\text{PH}_2\text{Ph})_2]$ (**3a**) and $[\text{Ru}^{\text{II}}(\text{Pc})(\text{P}(\text{HPh})_2)_2]$ (**4**) were prepared in 65% and 60% yields, respectively, by the reaction of $[\text{Ru}^{\text{II}}(\text{Pc})(\text{DMSO})_2]$ ¹¹ with PH_2Ph or $\text{P}(\text{HPh})_2$ (Scheme 2). In a previous work, we developed a one-pot synthesis of $[\text{Ru}^{\text{II}}(\text{Por})(\text{PH}_2\text{R})_2]$ from $\text{O}=\text{PCl}_2\text{R}$ or PCl_2R .^{7b} By extending this one-pot method to

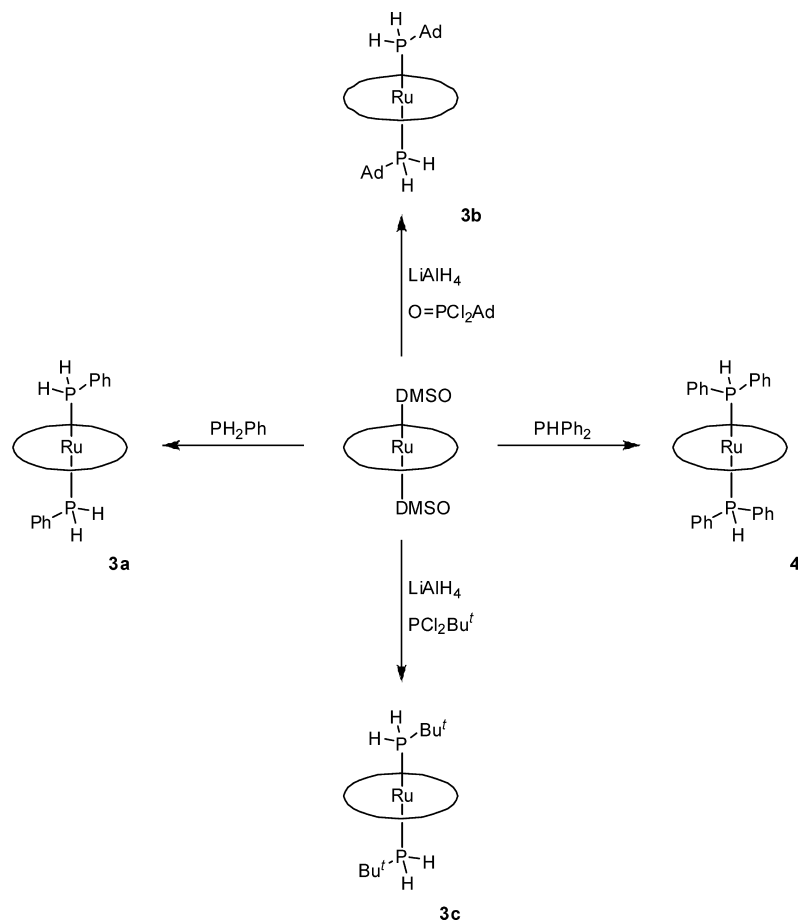
- (4) (a) Adachi, H.; Suzuki, H.; Miyazaki, Y.; Iimura, Y.; Hoshino, M. *Inorg. Chem.* **2002**, *41*, 2518. (b) Stulz, E.; Sanders, J. K. M.; Montalti, M.; Prodi, L.; Zaccheroni, N.; de Biani, F. F.; Grigiotti, E.; Zanello, P. *Inorg. Chem.* **2002**, *41*, 5269. (c) Suzuki, H.; Miyazaki, Y.; Hoshino, M. *J. Phys. Chem. A* **2003**, *107*, 1239. (d) Inamo, M.; Matsubara, N.; Nakajima, K.; Iwayama, T. S.; Okimi, H.; Hoshino, M. *Inorg. Chem.* **2005**, *44*, 6445.
- (5) (a) Stulz, E.; Ng, Y.-F.; Scott, S. M.; Sanders, J. K. M. *Chem. Commun.* **2002**, 524. (b) Stulz, E.; Maue, M.; Feeder, N.; Teat, S. J.; Ng, Y.-F.; Bond, A. D.; Darling, S. L.; Sanders, J. K. M. *Inorg. Chem.* **2002**, *41*, 5255. (c) Stulz, E.; Scott, S. M.; Bond, A. D.; Otto, S.; Sanders, J. K. M. *Inorg. Chem.* **2003**, *42*, 3086. (d) Stulz, E.; Scott, S. M.; Bond, A. D.; Teat, S. J.; Sanders, J. K. M. *Chem.—Eur. J.* **2003**, *9*, 6039.
- (6) Stulz, E.; Maue, M.; Scott, S. M.; Mann, B. E.; Sanders, J. K. M. *New J. Chem.* **2004**, *28*, 1066.
- (7) (a) Xie, J.; Huang, J.-S.; Zhu, N.; Zhou, Z.-Y.; Che, C.-M. *Chem.—Eur. J.* **2005**, *11*, 2405. (b) Huang, J.-S.; Yu, G.-A.; Xie, J.; Zhu, N.; Che, C.-M. *Inorg. Chem.* **2006**, *45*, 5724.
- (8) Che, C.-M.; Huang, J.-S. *Coord. Chem. Rev.* **2002**, *231*, 151.
- (9) (a) Au, S.-M.; Huang, J.-S.; Yu, W.-Y.; Fung, W.-H.; Che, C.-M. *J. Am. Chem. Soc.* **1999**, *121*, 9120. (b) Leung, S. K.-Y.; Tsui, W.-M.; Huang, J.-S.; Che, C.-M.; Liang, J.-L.; Zhu, N. *J. Am. Chem. Soc.* **2005**, *127*, 16629.

- (10) (a) Sweigart, D. A. *J. Chem. Soc., Dalton Trans.* **1976**, 1476. (b) Lever, A. B. P.; Wilshire, J. P. *Inorg. Chem.* **1978**, *17*, 1145. (c) Martinsen, J.; Miller, M.; Trojan, D.; Sweigart, D. A. *Inorg. Chem.* **1980**, *19*, 2162. (d) Labauze, G.; Raynor, J. B. *J. Chem. Soc., Dalton Trans.* **1981**, 590. (e) Doeff, M. M.; Sweigart, D. A. *Inorg. Chem.* **1981**, *20*, 1683. (f) Stynes, D. V.; Fletcher, D.; Chen, X. *Inorg. Chem.* **1986**, *25*, 3483. (g) Bulatov, A.; Knecht, S.; Subramanian, L. R.; Hanack, M. *Chem. Ber.* **1993**, *126*, 2565. (h) Goeldner, M.; Kienast, A.; Homborg, H. Z. *Anorg. Allg. Chem.* **1998**, *624*, 141. (i) Chen, M. J.; Utschig, L. M.; Rathke, J. W. *Inorg. Chem.* **1998**, *37*, 5786. (j) Chen, M. J.; Klingler, R. J.; Rathke, J. W. *J. Porphyrins Phthalocyanines* **2001**, *5*, 442.
- (11) Kobel, W.; Hanack, M. *Inorg. Chem.* **1986**, *25*, 103.

Scheme 1



Scheme 2



the phthalocyanine counterparts, we prepared $[\text{Ru}^{\text{II}}(\text{Pc})(\text{PH}_2\text{-Ad})_2]$ (**3b**) and $[\text{Ru}^{\text{II}}(\text{Pc})(\text{PH}_2\text{Bu}^t)_2]$ (**3c**) (both in 70% yield) starting from $\text{O}=\text{P}(\text{Cl})_2\text{Ad}$ and PCl_2Bu^t , respectively (Scheme 2).

Attempts to isolate PH_2R or PHR_2 complexes of iron phthalocyanine have not been successful. The reaction of $[\text{Fe}(\text{Pc})]$ (purchased from Aldrich) with excess PH_2Ph or PPh_2 in tetrahydrofuran afforded an unstable product which has not been clearly identified.

Compared with $[\text{Ru}^{\text{II}}(\text{Por})(\text{PH}_2\text{Ph})_2]$ and $[\text{Ru}^{\text{II}}(\text{Por})(\text{PPh}_2)_2]$,^{7a} the iron(II) counterparts **1** and **2** are much more air-sensitive. When 5,10,15,20-tetrakis(*p*-R-phenyl)porphyrins (R = H, TPP; Me, TTP; Cl, 4-Cl-TPP) were used, the corresponding iron(II) complexes of PH_2R or PPh_2 could not be isolated in a pure form.

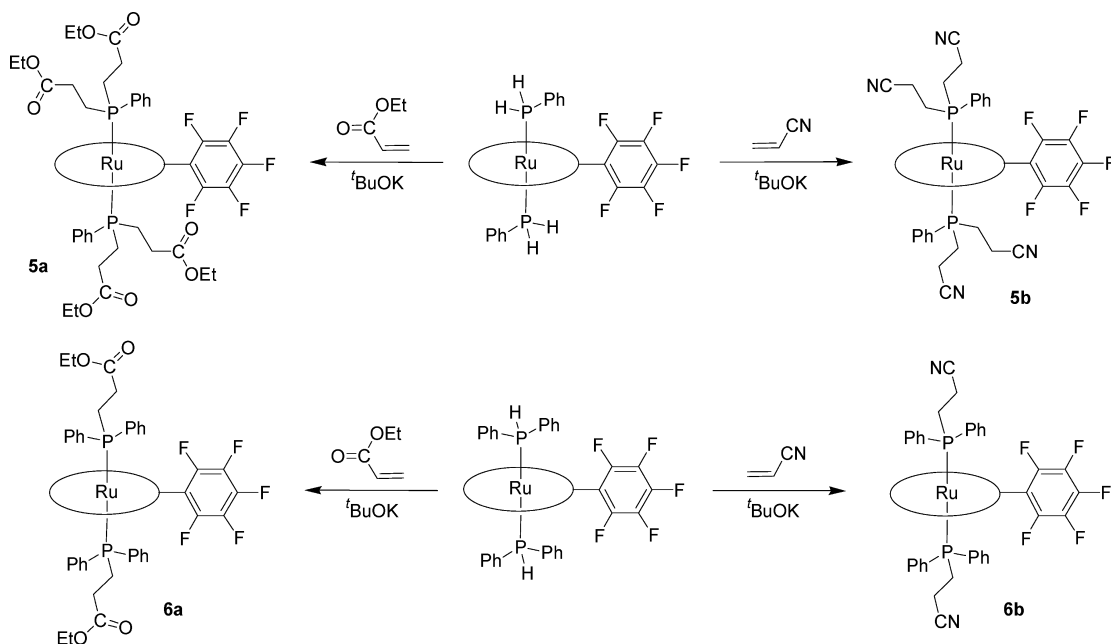
In contrast, the ruthenium(II) phthalocyanines **3** and **4** all exhibit a remarkable stability toward air in both the solid state and solution. The stability of $[\text{Ru}^{\text{II}}(\text{Pc})(\text{PH}_2\text{Ph})_2]$ (**3a**)

and $[\text{Ru}^{\text{II}}(\text{Pc})(\text{PPh}_2)_2]$ (**4**) is comparable to that of $[\text{Ru}^{\text{II}}(\text{F}_{20}\text{-TPP})(\text{PH}_2\text{Ph})_2]$ and $[\text{Ru}^{\text{II}}(\text{F}_{20}\text{-TPP})(\text{PPh}_2)_2]$; the latter complexes bear a fluorinated porphyrin ligand and were found to exhibit the highest stability among all previously reported PH_2R complexes of ruthenium porphyrins.⁷

Complexes **1–4** constitute new families of metal PH_2R and PHR_2 complexes. From the literature, we have not found other examples of primary or secondary phosphine complexes of iron porphyrins and metallophthalocyanines, despite the reports on a number of iron porphyrins¹² and metallophthalocyanines¹⁰ that bear tertiary phosphine axial ligands.

P–H Bond Functionalization. The P–H bonds of PH_2R and PHR_2 can be functionalized in several ways, including hydrophosphination with alkenes (or alkynes) and P-alkylation with haloalkanes. Isolated metal PH_2R or PHR_2 complexes that have been reported to undergo hydrophosphination¹³ or P-alkylation¹⁴ are sparse and are confined to metal carbonyls. Both the hydrophosphination and P-alky-

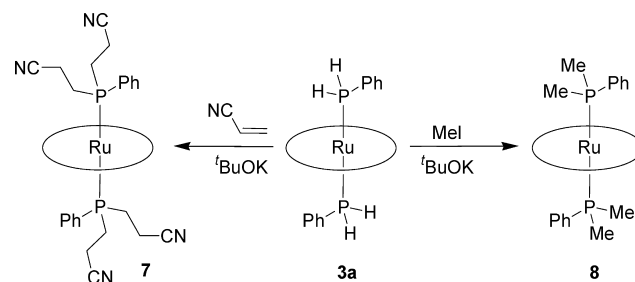
Scheme 3



lation reactions require the use of bases, such as $t\text{BuLi}$, KH , 1,8-diazabicyclo[5.4.0]undec-7-ene, and Et_3N , for the deprotonation of the coordinated PH_2R or PHR_2 to give the corresponding phosphido complexes. Reactions of isolated phosphido complexes of metal carbonyls with alkenes (or alkynes) and haloalkanes (or other alkyl cation sources) to afford hydrophosphination¹⁵ and P-alkylation¹⁶ products, respectively, have been documented. Phosphido complexes of platinum and ruthenium with di(tertiary phosphine) auxiliary ligands instead of carbonyls are also known to undergo hydrophosphination^{17a,b} and P-alkylation.^{17c,d,18}

Our efforts in functionalizing the P–H bonds coordinated to metal complexes were initially focused on alkene hydrophosphination by $[\text{Ru}^{\text{II}}(\text{F}_{20}\text{-TPP})(\text{PH}_2\text{Ph})_2]$ and $[\text{Ru}^{\text{II}}(\text{F}_{20}\text{-$

Scheme 4



$\text{TPP})(\text{PHPh}_2)_2]$. The iron(II) complexes **1** and **2** were not employed in such studies due to their high air-sensitivity. Treatment of $[\text{Ru}^{\text{II}}(\text{F}_{20}\text{-TPP})(\text{PH}_2\text{Ph})_2]$ with 4 equiv of $\text{CH}_2=\text{CHR}$ ($\text{R} = \text{CO}_2\text{Et}$, CN) and $t\text{BuOK}$ in acetone afforded $[\text{Ru}^{\text{II}}(\text{F}_{20}\text{-TPP})(\text{P}(\text{CH}_2\text{CH}_2\text{R})_2\text{Ph})_2]$ ($\text{R} = \text{CO}_2\text{Et}$, **5a**; CN , **5b**) in ~85% yields (Scheme 3). Similar reactions of $[\text{Ru}^{\text{II}}(\text{F}_{20}\text{-TPP})(\text{PHPh}_2)_2]$ with 2 equiv of $\text{CH}_2=\text{CHR}$ ($\text{R} = \text{CO}_2\text{Et}$, CN) and $t\text{BuOK}$ gave $[\text{Ru}^{\text{II}}(\text{F}_{20}\text{-TPP})(\text{P}(\text{CH}_2\text{CH}_2\text{R})\text{Ph})_2]$ ($\text{R} = \text{CO}_2\text{Et}$, **6a**; CN , **6b**) in ~80% yields (Scheme 3).

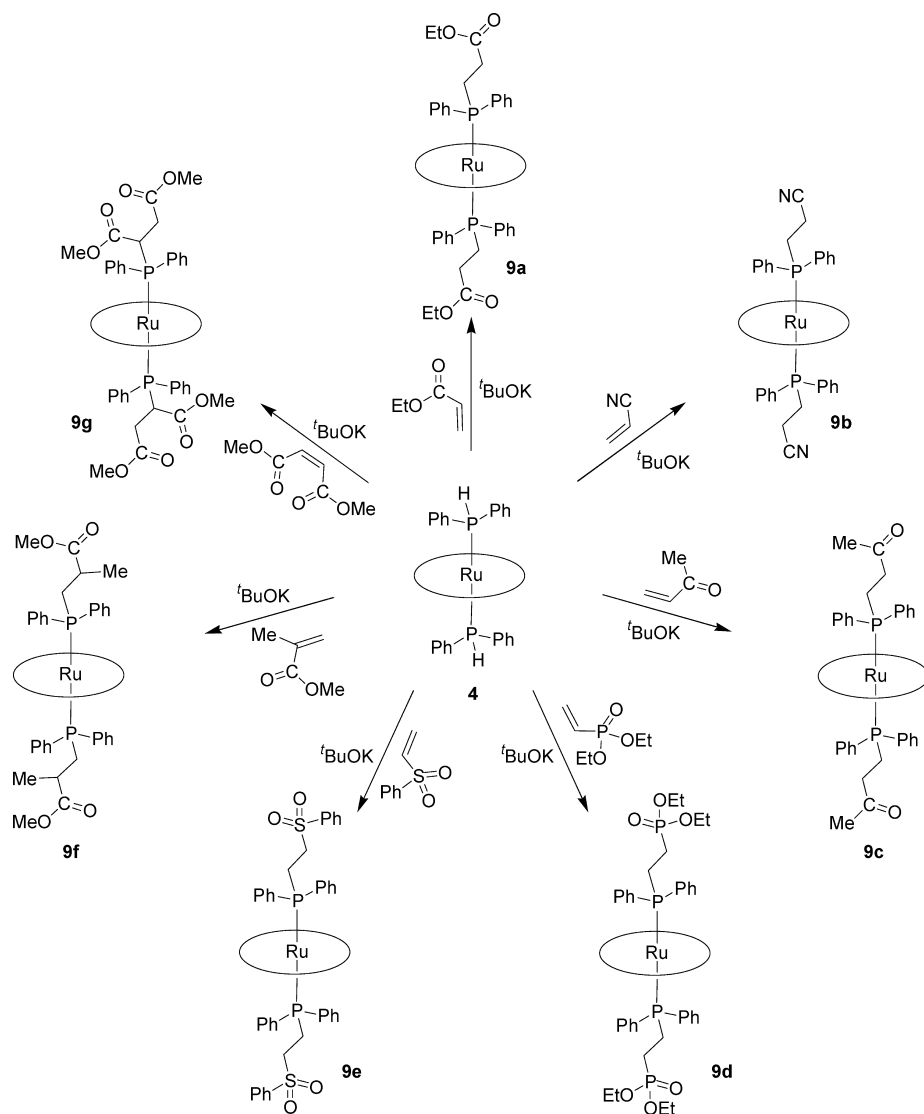
Upon isolation of the ruthenium(II) phthalocyanines **3a** and **4**, which can be obtained from PH_2Ph or PHPh_2 , RuCl_3 , and inexpensive phthalonitrile, we examined their reactivity toward P–H bond functionalization reactions.

Reaction of **3a** with excess $\text{CH}_2=\text{CHCN}$ and $t\text{BuOK}$ in tetrahydrofuran for 1 h resulted in the formation of $[\text{Ru}^{\text{II}}(\text{Pc})(\text{P}(\text{CH}_2\text{CH}_2\text{CN})_2\text{Ph})_2]$ (**7**; Scheme 4), which was isolated in 60% yield. When **3a** was treated with MeI , instead of $\text{CH}_2=\text{CHCN}$, under similar conditions, the P-alkylation

- (12) (a) Spiro, T. G.; Burke, J. M. *J. Am. Chem. Soc.* **1976**, *98*, 5482. (b) Connor, W. M.; Straub, D. K. *Inorg. Chem.* **1977**, *16*, 491. (c) Chin, D.-H.; La Mar, G. N.; Balch, A. L. *J. Am. Chem. Soc.* **1980**, *102*, 5945. (d) Dawson, J. H.; Andersson, L. A.; Sono, M. *J. Biol. Chem.* **1983**, *258*, 13637. (e) Ohya, T.; Morohoshi, H.; Sato, M. *Inorg. Chem.* **1984**, *23*, 1303. (f) Sono, M.; Dawson, J. H.; Hager, L. P. *Inorg. Chem.* **1985**, *24*, 4339. (g) Bondon, A.; Petrisko, P.; Sodano, P.; Simonneaux, G. *Biochim. Biophys. Acta* **1986**, *872*, 163. (h) Stynes, D. V.; Fletcher, D.; Chen, X. *Inorg. Chem.* **1986**, *25*, 3483. (i) Simonneaux, G.; Sodano, P. *J. Organomet. Chem.* **1988**, *349*, C11. (j) Sodano, P.; Simonneaux, G.; Toupet, L. *J. Chem. Soc., Dalton Trans.* **1988**, 2615. (k) Belani, R. M.; James, B. R.; Dolphin, D.; Rettig, S. J. *Can. J. Chem.* **1988**, *66*, 2072. (l) Simonneaux, G.; Sodano, P. *Inorg. Chem.* **1988**, *27*, 3956. (m) Toupet, L.; Sodano, P.; Simonneaux, G. *Acta Crystallogr., Sect. C* **1990**, *C46*, 1631. (n) Grodzicki, M.; Flint, H.; Winkler, H.; Walker, F. A.; Trautwein, A. X. *J. Phys. Chem. A* **1997**, *101*, 4202.
- (13) Malisch, W.; Klüpfel, B.; Schumacher, D.; Nieger, M. *J. Organomet. Chem.* **2002**, *661*, 95.
- (14) (a) Treichel, P. M.; Douglas, W. M.; Dean, W. K. *Inorg. Chem.* **1972**, *11*, 1615. (b) Adams, H.; Atkinson, M. T.; Morris, M. J. *J. Organomet. Chem.* **2001**, *633*, 125.
- (15) (a) Seyferth, D.; Wood, T. G. *Organometallics* **1987**, *6*, 2563. (b) Seyferth, D.; Wood, T. G. *Organometallics* **1988**, *7*, 714. (c) Sugiura, J.; Kakizawa, T.; Hashimoto, H.; Tobita, H.; Ogino, H. *Organometallics* **2005**, *24*, 1099.
- (16) (a) McNamara, W. F.; Reisacher, H.-U.; Duesler, E. N.; Paine, R. T. *Organometallics* **1988**, *7*, 1313. (b) Brunet, J.-J.; Chauvin, R.; Diallo, O.; Donnadiou, B.; Jaffart, J.; Neibecker, D. *J. Organomet. Chem.* **1998**, *570*, 195.

- (17) (a) Wicht, D. K.; Kourkine, I. V.; Lew, B. M.; Nthenge, J. M.; Glueck, D. S. *J. Am. Chem. Soc.* **1997**, *119*, 5039. (b) Scriban, C.; Glueck, D. S.; Zakharov, L. N.; Kassel, W. S.; DiPasquale, A. G.; Golen, J. A.; Rheingold, A. L. *Organometallics* **2006**, *25*, 5757. (c) Scriban, C.; Glueck, D. S. *J. Am. Chem. Soc.* **2006**, *128*, 2788. (d) Scriban, C.; Glueck, D. S.; Golen, J. A.; Rheingold, A. L. *Organometallics* **2007**, *26*, 1788.
- (18) Chan, V. S.; Stewart, I. C.; Bergman, R. G.; Toste, F. D. *J. Am. Chem. Soc.* **2006**, *128*, 2786.

Scheme 5



product $[\text{Ru}^{\text{II}}(\text{Pc})(\text{PMe}_2\text{Ph})_2]$ (**8**; Scheme 4) was obtained in ~50% isolated yield.

To examine the scope of the hydrophosphination and P-alkylation of the P–H bonds coordinated to a metallophthalocyanine, we focused the studies on complex **4** containing a secondary arylphosphine ligand. When **4** was treated with excess $\text{CH}_2=\text{CHR}$ ($\text{R} = \text{CO}_2\text{Et}$, CN) and $t\text{BuOK}$ in tetrahydrofuran for 1 h, the reactions afforded $[\text{Ru}^{\text{II}}(\text{Pc})(\text{P}(\text{CH}_2\text{CH}_2\text{R})\text{Ph}_2)_2]$ ($\text{R} = \text{CO}_2\text{Et}$, **9a**; CN , **9b**; Scheme 5) in ~70% yields. Under similar conditions, **4** also reacted with a series of other alkenes, including $\text{CH}_2=\text{CHC}(\text{O})\text{Me}$, $\text{CH}_2=\text{CHP}(\text{O})(\text{OEt})_2$, $\text{CH}_2=\text{CHS}(\text{O})_2\text{Ph}$, $\text{CH}_2=\text{C}(\text{Me})\text{CO}_2\text{Me}$, and $\text{CH}(\text{CO}_2\text{Me})=\text{CHCO}_2\text{Me}$, to give the corresponding hydrophosphination products $[\text{Ru}^{\text{II}}(\text{Pc})(\text{P}(\text{CH}_2\text{CH}_2\text{C}(\text{O})\text{Me})\text{Ph}_2)_2]$ (**9c**), $[\text{Ru}^{\text{II}}(\text{Pc})(\text{P}(\text{CH}_2\text{CH}_2\text{P}(\text{O})(\text{OEt})_2)\text{Ph}_2)_2]$ (**9d**), $[\text{Ru}^{\text{II}}(\text{Pc})(\text{P}(\text{CH}_2\text{CH}_2\text{S}(\text{O})_2\text{Ph})\text{Ph}_2)_2]$ (**9e**), $[\text{Ru}^{\text{II}}(\text{Pc})(\text{P}(\text{CH}_2\text{CH}(\text{Me})\text{CO}_2\text{Me})\text{Ph}_2)_2]$ (**9f**), and $[\text{Ru}^{\text{II}}(\text{Pc})(\text{P}(\text{CH}(\text{CO}_2\text{Me})\text{CH}_2\text{CO}_2\text{Me})\text{Ph}_2)_2]$ (**9g**; Scheme 5) in 56–76% yields.

Replacement of the alkenes in the foregoing reactions of **4** by MeI resulted in the isolation of $[\text{Ru}^{\text{II}}(\text{Pc})(\text{PMePh}_2)_2]$ (**10a**; Scheme 6) in 87% yield. This P-alkylation reaction

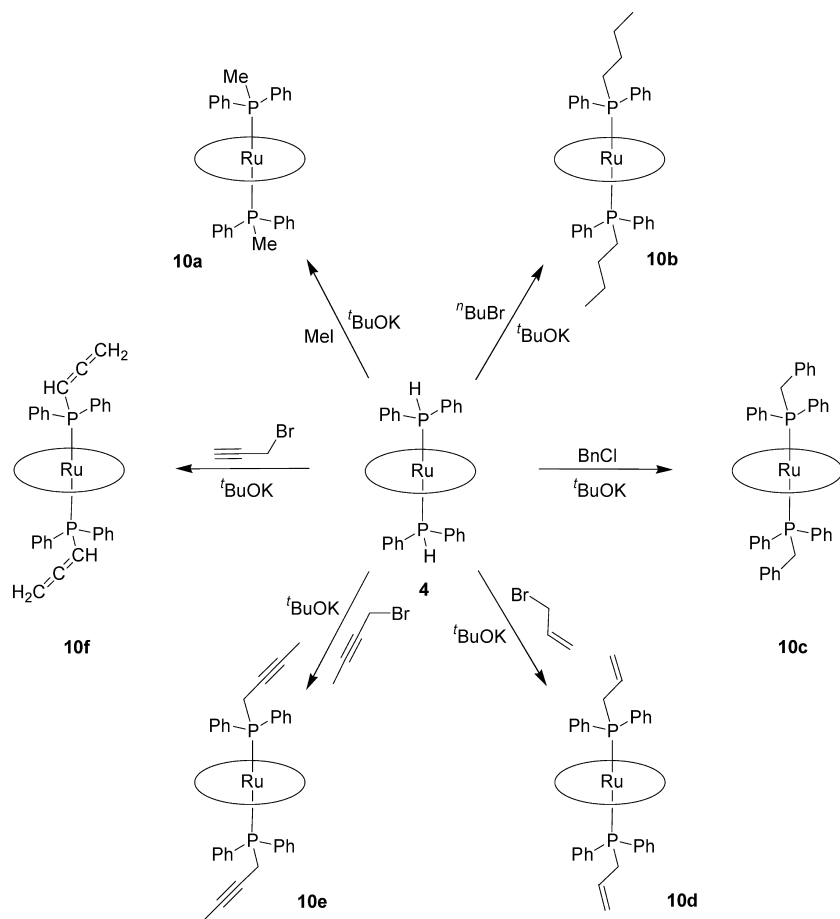
could be extended to other haloalkanes such as $t\text{BuBr}$ and BnCl ($\text{Bn} = \text{benzyl}$), producing $[\text{Ru}^{\text{II}}(\text{Pc})(\text{PRPh}_2)_2]$ ($\text{R} = \text{Bu}^t$, **10b**; Bn , **10c**; Scheme 6) in 50% and 62% yields, respectively.

We also examined the reactivity of **4** toward haloalkenes and haloalkynes. Treatment of **4** with excess allylbromide and $t\text{BuOK}$ in tetrahydrofuran gave $[\text{Ru}^{\text{II}}(\text{Pc})(\text{P}(\text{CH}_2\text{CH}=\text{CH}_2)\text{Ph}_2)_2]$ (**10d**; Scheme 6) in 60% yield. No hydrophosphination of the alkene group in allylbromide was observed. The reaction of **4** with excess $\text{MeC}\equiv\text{CCH}_2\text{Br}$ and $t\text{BuOK}$ afforded $[\text{Ru}^{\text{II}}(\text{Pc})(\text{P}(\text{CH}_2\text{C}\equiv\text{CMe})\text{Ph}_2)_2]$ (**10e**; Scheme 6) in 58% yield. Replacing $\text{MeC}\equiv\text{CCH}_2\text{Br}$ with propargylbromide in the reaction led to the isolation of $[\text{Ru}^{\text{II}}(\text{Pc})(\text{P}(\text{CH}=\text{C}=\text{CH}_2)\text{Ph}_2)_2]$ (**10f**; yield, 44%; Scheme 6), other than $[\text{Ru}^{\text{II}}(\text{Pc})(\text{P}(\text{CH}_2\text{C}\equiv\text{CH})\text{Ph}_2)_2]$; analogous propargyl-allenyl rearrangements have been reported in the literature.¹⁹

The reactions depicted in Schemes 4–6 demonstrate a facile approach to ruthenium phthalocyanines bearing a variety of tertiary phosphine axial ligands, of which, to the best of our knowledge, the free sulfonyl phosphine

(19) Alcaide, B.; Almendros, P.; Aragoncillo, C.; Rodríguez-Acebes, R. *Synthesis* **2003**, 1163.

Scheme 6



$\text{P}(\text{CH}_2\text{CH}_2\text{S}(\text{O})_2\text{Ph})\text{Ph}_2$ has not been reported previously, and the $\text{P}(\text{CH}_2\text{CH}_2\text{C}(\text{O})\text{Me})\text{Ph}_2$ and $\text{P}(\text{CH}_2\text{CH}(\text{Me})\text{CO}_2\text{Me})\text{Ph}_2$ ligands have not been documented to bind metal ions. We found that a direct reaction of $[\text{Ru}^{\text{II}}(\text{Pc})(\text{DMSO})_2]$ with excess $\text{P}(\text{CH}(\text{CO}_2\text{Me})\text{CH}_2\text{CO}_2\text{Me})\text{Ph}_2$ in dichloromethane for 2 h gave a mixture of products, from which **9g** could not be isolated in a pure form.

In the absence of $t\text{BuOK}$, neither a hydrophosphination nor a P-alkylation reaction was observed for the PH_2Ph and PPhPh_2 complexes of ruthenium(II) porphyrin and ruthenium(II) phthalocyanine. This suggests that the P–H bond functionalization reactions require in situ generation of the corresponding phosphido complexes. Our attempts to isolate the $(\text{PPh})^-$ or $(\text{PPh}_2)^-$ complexes of a ruthenium porphyrin or ruthenium phthalocyanine from the reaction of $[\text{Ru}^{\text{II}}(\text{F}_{20}\text{-TPP})(\text{PH}_2\text{Ph})_2]$, $[\text{Ru}^{\text{II}}(\text{F}_{20}\text{-TPP})(\text{PPhPh}_2)_2]$, **3a**, or **4** with $t\text{BuOK}$ have not been successful.

Spectral Features. i. NMR. Complexes **1–10** exhibit diamagnetic NMR spectra, as expected for low-spin d^6 iron(II) and ruthenium(II) complexes. The ^1H NMR spectra of the porphyrin complexes **1**, **2**, **5**, and **6** show pyrrolic proton resonances (H_β) as a singlet in the δ range of 8.09–8.60; the phthalocyanine complexes **3**, **4**, and **7–10** exhibit the proton resonances of the phthalocyanine ligand as two multiplets at $\delta \sim 9.0$ and ~ 7.9 . The phosphine ligands in **1–10**, excluding **1b** and **3b,c**, each bear at least one P-phenyl group; the proton resonances

of these phenyl groups appear as a single set of three signals (H_p , δ 6.63–6.94; H_m , δ 6.21–6.67; H_o , δ 4.11–4.68), except for **9g** (see below).

At room temperature, the ^1H and ^{31}P NMR spectra of $[\text{Fe}^{\text{II}}(\text{F}_{20}\text{-TPP})(\text{PH}_2\text{R})_2]$ (**1a,b**) in CDCl_3 solution show broad signals, unlike those of their ruthenium analogues.⁷ The ^1H NMR spectrum of **1a** is depicted in Figure 1 as an example. We suggest that there is a rapid exchange of PH_2Ph between its free and coordinated forms upon dissolving **1a** in a CDCl_3 solution. Indeed, lowering the temperature to -25°C markedly sharpens the NMR signals, resulting in the appearance of a signal pattern (for both ^1H and ^{31}P NMR, Figure 1) similar to that of $[\text{Ru}^{\text{II}}(\text{F}_{20}\text{-TPP})(\text{PH}_2\text{Ph})_2]$.^{7a} This indicates that, at low temperatures ($< -25^\circ\text{C}$), **1a** undergoes no significant phosphine dissociation in solution at an NMR concentration (~ 1 mM) and on the NMR time scale.

Compared with **1a,b**, $[\text{Fe}^{\text{II}}(\text{F}_{20}\text{-TPP})(\text{PPhPh}_2)_2]$ (**2a**) is more inert. In a CDCl_3 solution of **2a** at the NMR concentration (~ 1 mM), no significant dissociation of the coordinated PPhPh_2 occurs at room temperature on the NMR time scale, as revealed by its ^1H and ^{31}P NMR spectra that closely resemble those of $[\text{Ru}^{\text{II}}(\text{F}_{20}\text{-TPP})(\text{PPhPh}_2)_2]$.^{7a} Replacement of the $\text{F}_{20}\text{-TPP}$ ligand in **2a** with 2,6- Cl_2TPP markedly labilizes the complex in solution, since the ^1H NMR spectrum of **2b** in the PH signal region is almost featureless at room temperature, although such signals are well-resolved at -25°C .

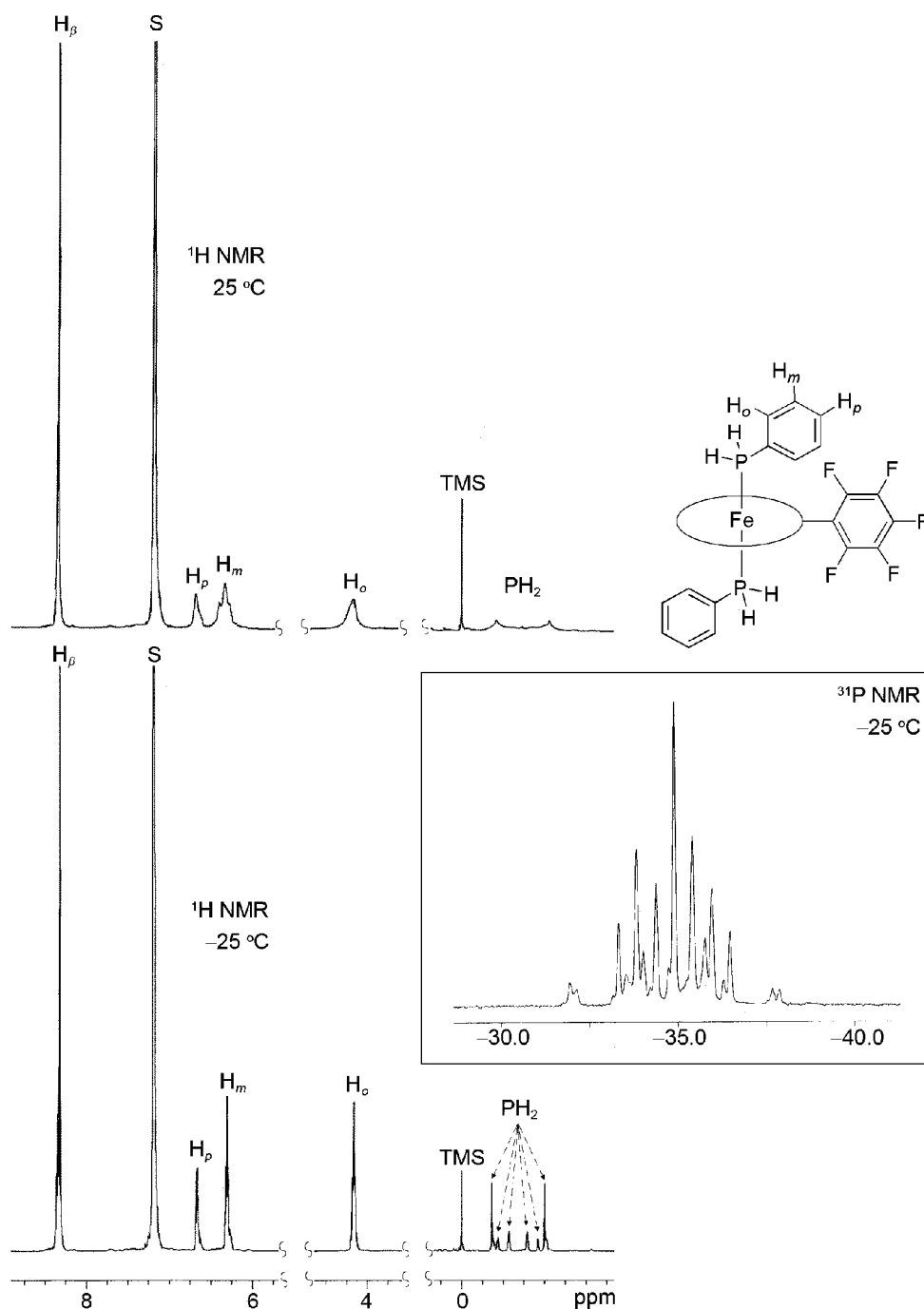


Figure 1. ^1H NMR spectra of **1a** in CDCl_3 at +25 and -25 °C. Inset: ^{31}P NMR spectrum of **1a** in CDCl_3 at -25 °C.

Ruthenium(II) phthalocyanines **3a–c** and **4** all remain intact in CDCl_3 solutions at room temperature for at least several days; their axial phosphine signals in the ^1H and ^{31}P NMR spectra are similar to those of the corresponding complexes of ruthenium(II) porphyrins.⁷ Figure 2 depicts the PH_2 or PH signals in the ^1H NMR spectra of **3a,c** and **4** and the ^{31}P NMR spectra of the same complexes. Heating a CDCl_3 solution of **3a** open to the air to 60 °C for 30 min did not cause any appreciable change in its ^1H and ^{31}P NMR spectra, revealing a remarkable stability of this primary phosphine complex.

The room-temperature ^1H NMR spectra of **5–10** in CDCl_3 solutions reveal no detectable dissociation of the coordinated

tertiary phosphines. For $\text{P}(\text{CH}_2\text{CH}_2\text{R})_2\text{Ph}$ ($\text{R} = \text{CO}_2\text{Et}$, CN) complexes **5a,b**, and **7**, the two protons in each methylene group ($\text{H}_{a,b}$ or $\text{H}_{c,d}$) of the phosphine ligands are diastereotopic and give different signals, as depicted in Figure S1 (see the Supporting Information) for **5b**, which features a set of four multiplets arising from H_{a-d} . In contrast, only two multiplets were observed for the corresponding methylene protons in the $\text{P}(\text{CH}_2\text{CH}_2\text{R})\text{Ph}_2$ complexes **6a,b** and **9a–e** (see Figure S1 for **6b** and Figure 3 for **9d**), since the two protons in each of these methylene group are equivalent. The appearance of the methylene signals in the high-field region is due to the ring current effect of the porphyrin or phthalocyanine ligand.

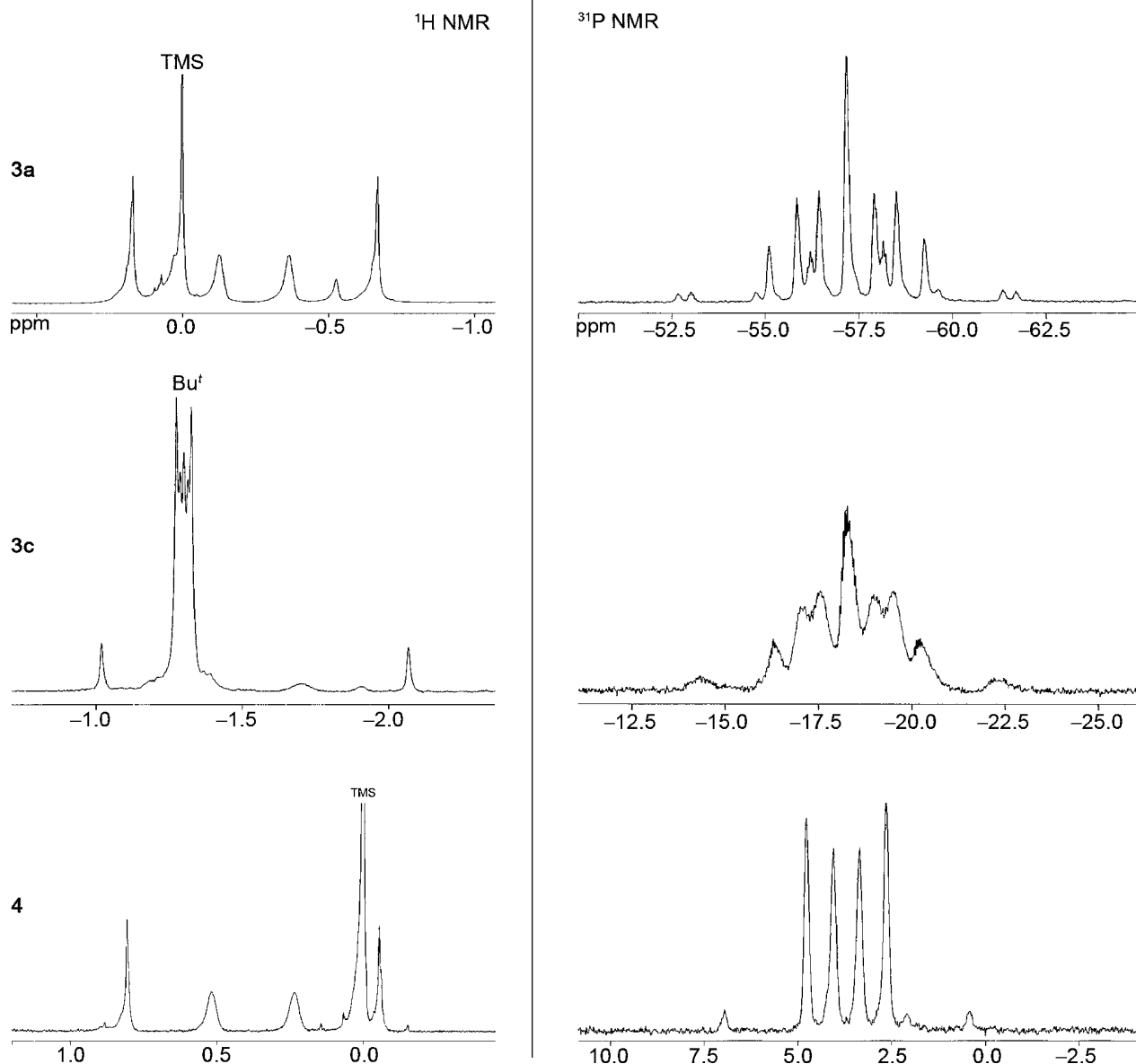


Figure 2. ^1H NMR spectra (in the P–H regions) and ^{31}P NMR spectra of **3a,c** and **4** in CDCl_3 . Some of the P–H signals of **3a,c** overlap with the TMS and Bu^t signals, respectively.

Complexes **9f** and **9g** have axial $\text{P}(\text{CH}_2\text{CH}(\text{Me})\text{CO}_2\text{Me})\text{Ph}_2$ and $\text{P}(\text{CH}(\text{CO}_2\text{Me})\text{CH}_2\text{CO}_2\text{Me})\text{Ph}_2$ ligands, respectively. Each of the tertiary diphenylphosphines has a methylene group and a methine group; the two protons of the methylene group are diastereotopic, and so are the two phenyl groups. As a result, two well-separated sets of phenyl signals, along with two multiplets from the methylene protons, appear in the ^1H NMR spectrum of **9g** (Figure 3). For **9f**, the methylene proton resonances appear as two multiplets, but there is only a single set of phenyl signals (Figure 3), probably owing to longer distances of the phenyl protons to the asymmetric methine C atom.

P-alkylation products **8** and **10a–c** do not contain diastereotopic methylene protons, like **6a,b** and **9a–e**. The R signals of the PRPh_2 ligands in **10b** ($\text{R} = \text{Bu}^t$), as compared with those in **10d** ($\text{R} = \text{CH}_2\text{CH}=\text{CH}_2$), **10e** ($\text{R} = \text{CH}_2\text{C}=\text{CMe}$), and **10f** ($\text{R} = \text{CH}=\text{C}=\text{CH}_2$), are shown in Figure 4. Complexes **10b,d,e** each have a P-methylene group,

whose signal appears at lower fields for **10d,e** than for **10b**. In contrast, no P-methylene signal similar to that of **10e** is observed for **10f** (Figure 4), which precludes formulation of **10f** as a $\text{P}(\text{CH}_2\text{C}\equiv\text{CH})\text{Ph}_2$ complex.

The $^{31}\text{P}\{^1\text{H}\}$ NMR spectra of **1–10** show the phosphine ^{31}P signal as a singlet, except for **9d** (which gives the corresponding signal as a triplet due to the presence of a $\text{P}(\text{O})(\text{OEt})_2$ group). For $[\text{M}^{\text{II}}(\text{F}_{20}\text{-TPP})(\text{PH}_2\text{Ph})_2]$ with $\text{M} = \text{Fe}$ (**1a**) and Ru,^{7a} the ^{31}P signal appears at $\delta -34.8$ and -55.2 , respectively, both at a lower field than that of $[\text{Ru}^{\text{II}}(\text{Pc})(\text{PH}_2\text{Ph})_2]$ (**3a**) with $\delta -57.2$. This trend of chemical shifts ($\text{Fe} > \text{Ru}$, $\text{F}_{20}\text{-TPP} > \text{Pc}$) is parallel to those observed for the secondary phosphine complexes $[\text{M}^{\text{II}}(\text{F}_{20}\text{-TPP})(\text{PH}-$

(20) Rawling, T.; McDonagh, A. *Coord. Chem. Rev.* **2007**, *251*, 1128.

(21) Ball, R. G.; Domazetis, G.; Dolphin, D.; James, B. R.; Trotter, J. *Inorg. Chem.* **1981**, *20*, 1556.

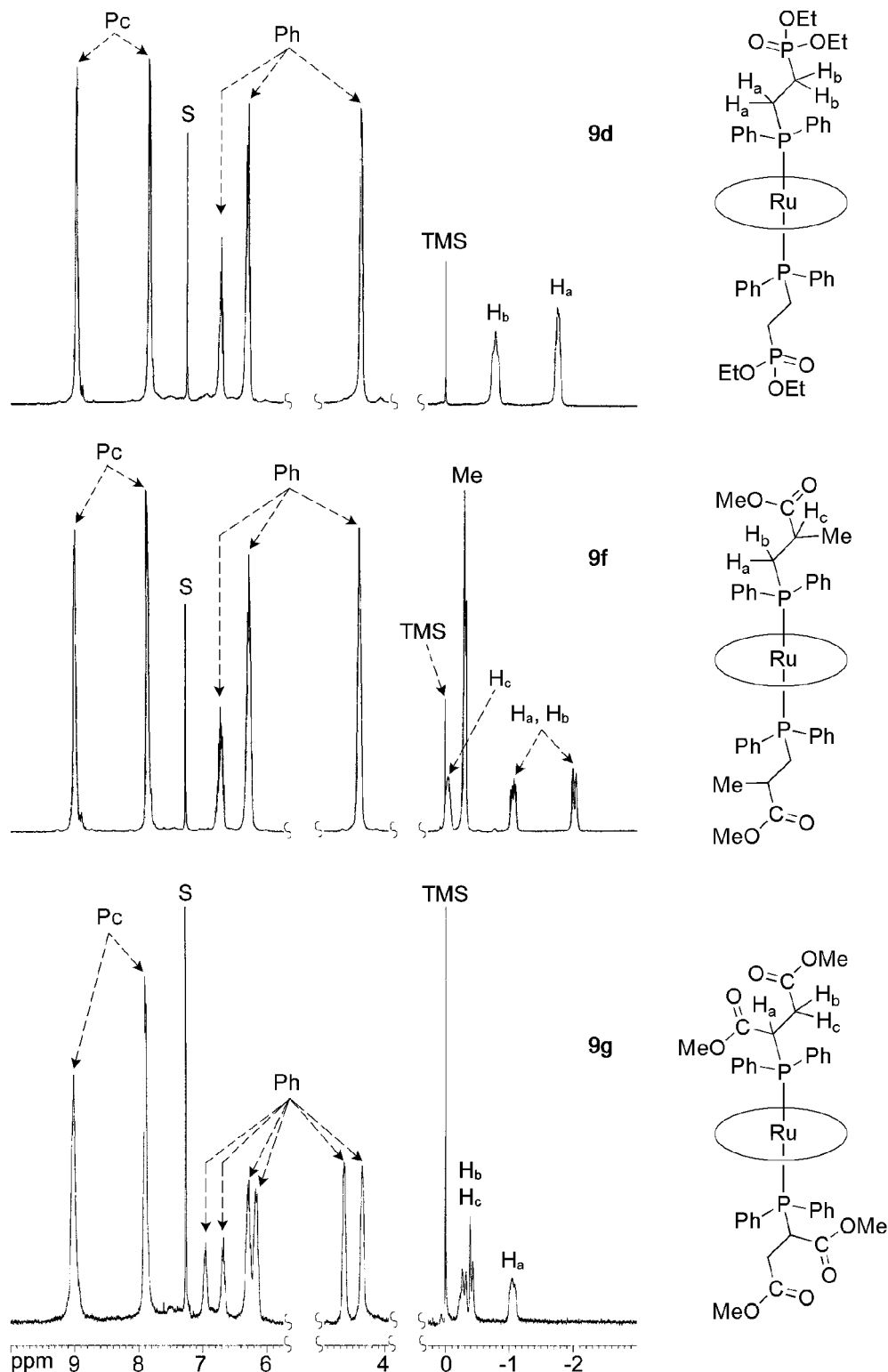


Figure 3. ^1H NMR spectra of **9d,f,g** in CDCl_3 showing the signals of phthalocyanine (Pc) and the axial phosphine ligands except those of the OMe or OEt groups.

$\text{Ph}_2)_2]$ ($\text{M} = \text{Fe}$ (**2a**), δ 21.7; Ru , δ 9.9^{7a}) and $[\text{Ru}^{\text{II}}(\text{Pc})(\text{PPh}_2)_2]$ (**4**, δ 3.7). The phosphine ^{31}P chemical shifts (δ) of **5–10** range from -1.3 to $+16.2$.

ii. UV–Vis Spectroscopy and Mass Spectrometry. Six-coordinate ruthenium phthalocyanines are known to exhibit an intense Soret band at $300\text{--}325$ nm and an intense Q band at $620\text{--}652$ nm, together with two weaker shoulder bands

at $340\text{--}385$ nm and $560\text{--}595$ nm, in their UV–vis spectra.²⁰ Similar UV–vis spectra were observed for **3**, **4**, and **7–10**. For **5** and **6**, their UV–vis spectra show Soret and β bands at $433\text{--}439$ and $518\text{--}524$ nm, respectively, which are typical for tertiary phosphine complexes of ruthenium *meso*-tetraarylporphyrins.²¹ The UV–vis spectra of **1** and **2** were obtained under nitrogen in the presence of an excess of the

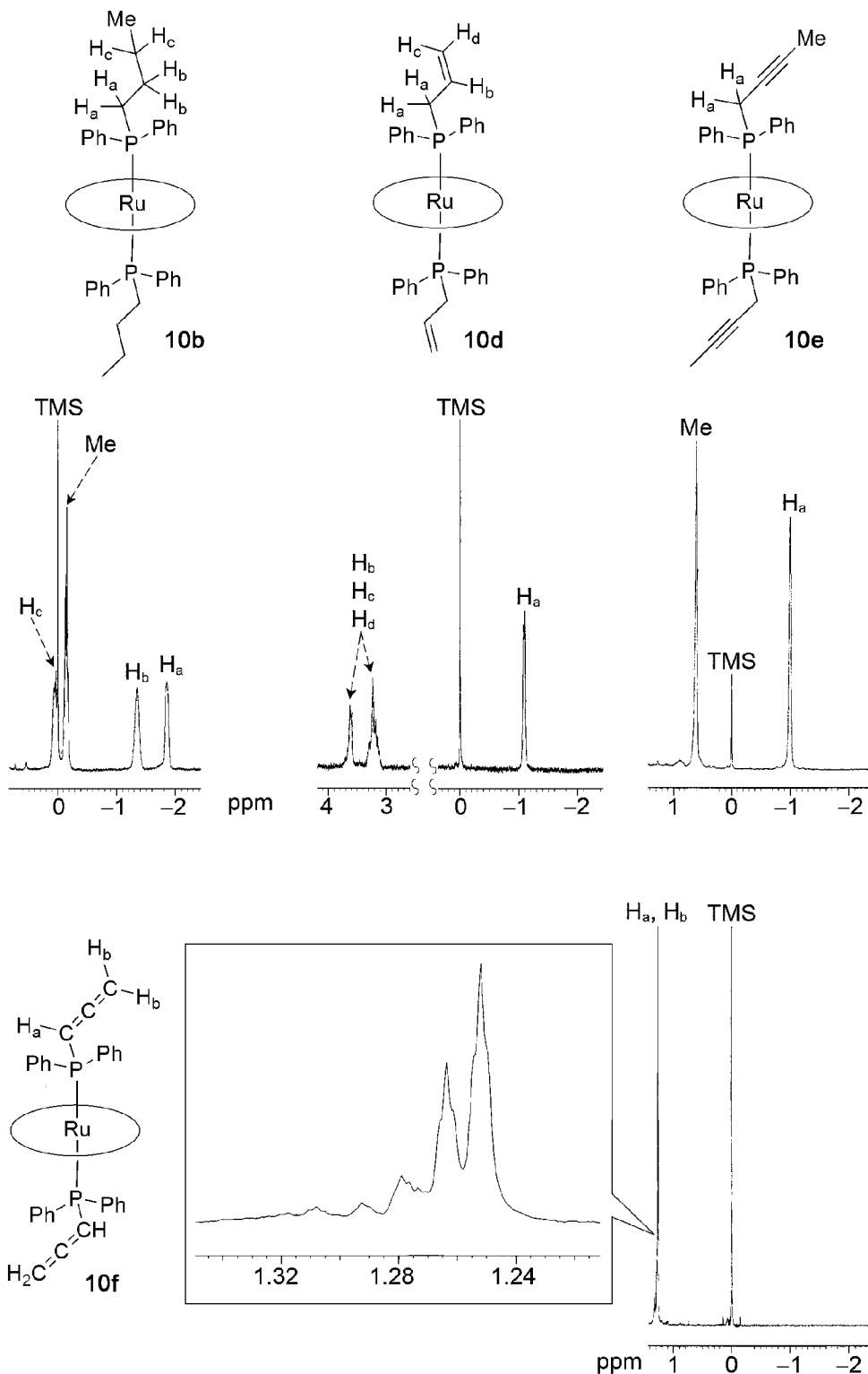


Figure 4. ^1H NMR spectra of **10b,d,e,f** in CDCl_3 showing the signals of the axial phosphine ligands except those of the phenyl groups. The inset is an enlargement of the $\text{H}_{a,b}$ signal for **10f**.

corresponding free PH_2R or PPhPh_2 , owing to the lability and high air sensitivity of these complexes in solutions at room temperature. The Soret bands (448–454 nm) and β bands (546–552 nm) of **1** and **2** are comparable to those (Soret 450 nm, β 550 nm) of $[\text{Fe}^{\text{II}}(\text{TPP})(\text{PPh}_3)_2]$ (TPP = 5,10,15,20-tetraphenylporphyrinato dianion).^{12k}

In the mass spectra of **1–10**, there are peaks that can be assigned to the parent ions M^+ and the fragments $[\text{M}-\text{L}]^+$

and $[\text{M}-2\text{L}]^+$, where L is the corresponding phosphine ligand in these complexes.

X-Ray Crystal Structural Determination. We have obtained diffraction-quality crystals of **1a**, **2b**· $2\text{CH}_2\text{Cl}_2$, **3b,c**, **4**, and **5b**· $2\text{CH}_2\text{Cl}_2$ and determined their structures by X-ray crystallography. The crystallographic data are compiled in Tables 1 and 2, and the ORTEP drawings of the structures, which all feature a planar porphyrin or phthalocyanine ring

Table 1. Crystallographic Data of Porphyrin Complexes **1a**, **2b**·2CH₂Cl₂, and **5b**·2CH₂Cl₂

	1a	2b ·2CH ₂ Cl ₂	5b ·2CH ₂ Cl ₂
formula	C ₅₆ H ₂₂ F ₂₀ FeN ₄ P ₂	C ₇₀ H ₄₄ Cl ₁₂ FeN ₄ P ₂	C ₇₂ H ₄₂ Cl ₈ F ₂₀ N ₈ P ₂ Ru
cryst syst	monoclinic	triclinic	monoclinic
fw	1248.57	1484.28	1845.75
space group	<i>P</i> 2 ₁ / <i>c</i>	<i>P</i> $\bar{1}$	<i>P</i> 2 ₁ / <i>c</i>
<i>a</i> , Å	13.000(3)	12.279(4)	13.205(3)
<i>b</i> , Å	7.7410(15)	12.517(4)	19.241(4)
<i>c</i> , Å	25.641(5)	12.727(4)	15.281(3)
α , deg	90.00	91.57(3)	90.00
β , deg	102.49(3)	107.00(3)	111.03(3)
γ , deg	90.00	117.49(3)	90.00
<i>V</i> , Å ³	2519.3(9)	1628.7(9)	3623.9(13)
<i>Z</i>	2	1	2
ρ_{calcd} , g cm ⁻³	1.646	1.513	1.691
2 θ range, deg	51.28	55.14	51.28
GOF	1.03	1.08	1.13
<i>R</i> 1/ <i>wR</i> 2	0.045/0.119	0.093/0.206	0.057/0.171

Table 2. Crystallographic Data of Phthalocyanine Complexes **3b**, **3c**, and **4**

	3b	3c	4
formula	C ₅₂ H ₄₆ N ₈ P ₂ Ru	C ₄₀ H ₆₀ N ₈ P ₂ Ru	C ₅₆ H ₃₈ N ₈ P ₂ Ru
cryst syst	monoclinic	monoclinic	triclinic
fw	945.98	793.79	985.95
space group	<i>P</i> 2 ₁ / <i>c</i>	<i>P</i> 2 ₁ / <i>c</i>	<i>P</i> $\bar{1}$
<i>a</i> , Å	12.063(2)	17.976(4)	12.739(3)
<i>b</i> , Å	12.717(2)	11.971(3)	12.791(3)
<i>c</i> , Å	18.652(4)	18.811(4)	15.547(3)
α , deg	90.00	90.00	107.99(3)
β , deg	92.15(3) ^o	111.83(3)	101.17(3)
γ , deg	90.00	90.00	97.94(3)
<i>V</i> , Å ³	2859.3(9)	3757.7(15)	2310.0(8)
<i>Z</i>	2	4	2
ρ_{calc} , g cm ⁻³	1.099	1.403	1.418
2 θ range, deg	51.32	51.28	51.76
GOF	0.98	0.91	0.98
<i>R</i> 1/ <i>wR</i> 2	0.069/0.187	0.061/0.169	0.035/0.084

and a crystallographic center of symmetry, are shown in Figure 5. A comparison of the average geometrical parameters among these complexes and previously reported iron(II)^{12j,k} and ruthenium(II)^{7,21,22} porphyrin analogues is given in Table 3.

For [M^{II}(F₂₀-TPP)(PH₂Ph)₂] (M = Fe (**1a**), Ru^{7a}), the M–P distances (M = Fe, 2.2597(9); Ru, 2.3603(10) Å), M–N distances (M = Fe, 1.998(2); Ru, 2.055(2) Å), P–C distances (M = Fe, 1.803(4); Ru, 1.824(3) Å), and M–P–C angles (M = Fe, 120.31(11)^o; Ru, 129.11(11)^o) follow an order of Fe < Ru. A similar order was observed by comparing the M–P and M–N distances of **2b** (M = Fe) with those of [Ru^{II}(F₂₀-TPP)(PHPh₂)₂]^{7a} and [Ru^{II}(4-Cl-TPP)(PHPh₂)₂]^{7a}; the former has a similar P–C distance and a slightly larger M–P–C angle compared with the latter two ruthenium analogues.

Prior to this work, no phosphine complex of a ruthenium phthalocyanine has been structurally characterized by X-ray crystallography, and the reported crystal structures of ruthenium phthalocyanines are sparse.²⁰ From the average geometric parameters of [Ru^{II}(L)(PH₂Ad)₂] (L = Pc (**3b**), TTP^{7b}) and [Ru^{II}(L)(PHPh₂)₂] (L = Pc (**4**), 4-Cl-TPP,^{7a} F₂₀-TPP^{7a}), it is evident that the phthalocyanine complexes **3b** and **4** have comparable Ru–P distances (2.3478(11)–2.3707(13) Å) and slightly shorter Ru–N distances (2.007(4)–2.016(2) Å) relative to those of their porphyrin analogues (Ru–P, 2.3397(11)–2.3516(13) Å; Ru–N, 2.050(3)–2.055(45)

Å). The P–C distance (1.844(5) Å) and Ru–P–C angle (128.50(16)^o) of [Ru^{II}(L)(PH₂Ad)₂] for L = Pc (**3b**) are almost identical to the corresponding values for L = TTP (P–C, 1.844(21) Å; Ru–P–C, 128.34(10)^o).^{7b}

Complex **5b** has a Ru–P distance of 2.3754(10) Å, slightly longer than that of 2.3603(10) Å in [Ru^{II}(F₂₀-TPP)(PH₂Ph)₂]^{7a} but shorter than those in [Ru^{II}(TPP)(PPH₂CH₂PPh₂)₂] (2.398(3) Å),²¹ [Ru^{II}(F₂₀-TPP)(PPh₃)₂] (2.4643(9) Å),²² and [Ru^{II}(F₂₈-TPP)(PPh₃)₂] (2.4807(7) Å, F₂₈-TPP = 2,3,7,8,12,13,17,18-octafluoro-5,10,15,20-tetrakis(pentafluorophenyl)porphyrinato dianion).²² Likewise, the Fe–P distances in [Fe^{II}(TPP)(PMe₂Ph)₂] (2.284(1) Å)^{12j} and [Fe^{II}(TPP)(PBuⁿ)₃] (2.3457(11) Å)^{12k} are longer than that in the PH₂Ph complex **1a**. Considerably smaller M–P–C angles are found in the tertiary phosphine complexes listed in Table 3 relative to the PH₂R or PHPh₂ complexes **1a**, **2b**, **3b,c**, and **4**, regardless of whether M = Fe or Ru, and whether the auxiliary ligand is porphyrin or phthalocyanine.

Notably, in the crystal structures of the phthalocyanine complexes **3c** and **4**, there are intermolecular C–H⋯ π interactions, as depicted in Figure 6. Both **3c** and **4** have two independent types of molecules (A and B) in the respective crystal structure, and the C–H⋯ π interactions (close H⋯C distances: 2.726–2.795 Å in **3c**, 2.615–2.780 Å in **4**) link each molecule A with four molecules B, and vice versa. Such a linkage of molecules by C–H⋯ π interactions generates a 3D network for **3c** but 2D sheets for **4**; no significant C–H⋯ π interactions are present between the 2D sheets of the latter complex.

Conclusion

We have isolated and characterized several primary and secondary phosphine complexes of iron(II) porphyrins and ruthenium(II) phthalocyanine, of which the iron complexes are highly air-sensitive, but the ruthenium phthalocyanine complexes are remarkably stable toward air in both the solid state and solution. The PH₂Ph and PHPh₂ stabilized by ruthenium phthalocyanine, and by ruthenium porphyrin F₂₀-TPP as well, can undergo hydrophosphination reactions with alkenes or P-alkylation with halo compounds. Through such P–H bond functionalization reactions, ruthenium phthalocyanine complexes of a variety of tertiary phosphines bearing alkoxy-carbonyl, cyano, ketyl, alkoxyphosphonyl, sulfonyl, alkene, alkyne, and allene functional groups could be isolated.

Experimental Section

General. All manipulations were performed under argon or nitrogen by using standard Schlenk technique unless otherwise specified. Dichloromethane and hexane were purified by a solvent purification system (Innovative technology, Inc.). Tetrahydrofuran (THF) and cyclohexane were distilled from CaH₂; methanol was distilled from magnesium/iodine. O=P(Cl)₂Ad,²³ [Ru^{II}(F₂₀-TPP)(PH₂Ph)₂]^{7a}, [Ru^{II}(F₂₀-TPP)(PHPh₂)₂]^{7a}, and [Ru^{II}(Pc)(DM-SO)₂]¹¹ were prepared by literature methods. Other reagents were

(22) Che, C.-M.; Zhang, J.-L.; Zhang, R.; Huang, J.-S.; Lai, T.-S.; Tsui, W.-M.; Zhou, X.-G.; Zhou, Z.-Y.; Zhu, N.; Chang, C. K. *Chem.-Eur. J.* **2005**, *11*, 7040.

(23) Stetter, H.; Last, W. D. *Chem. Ber.* **1969**, *102*, 3364.

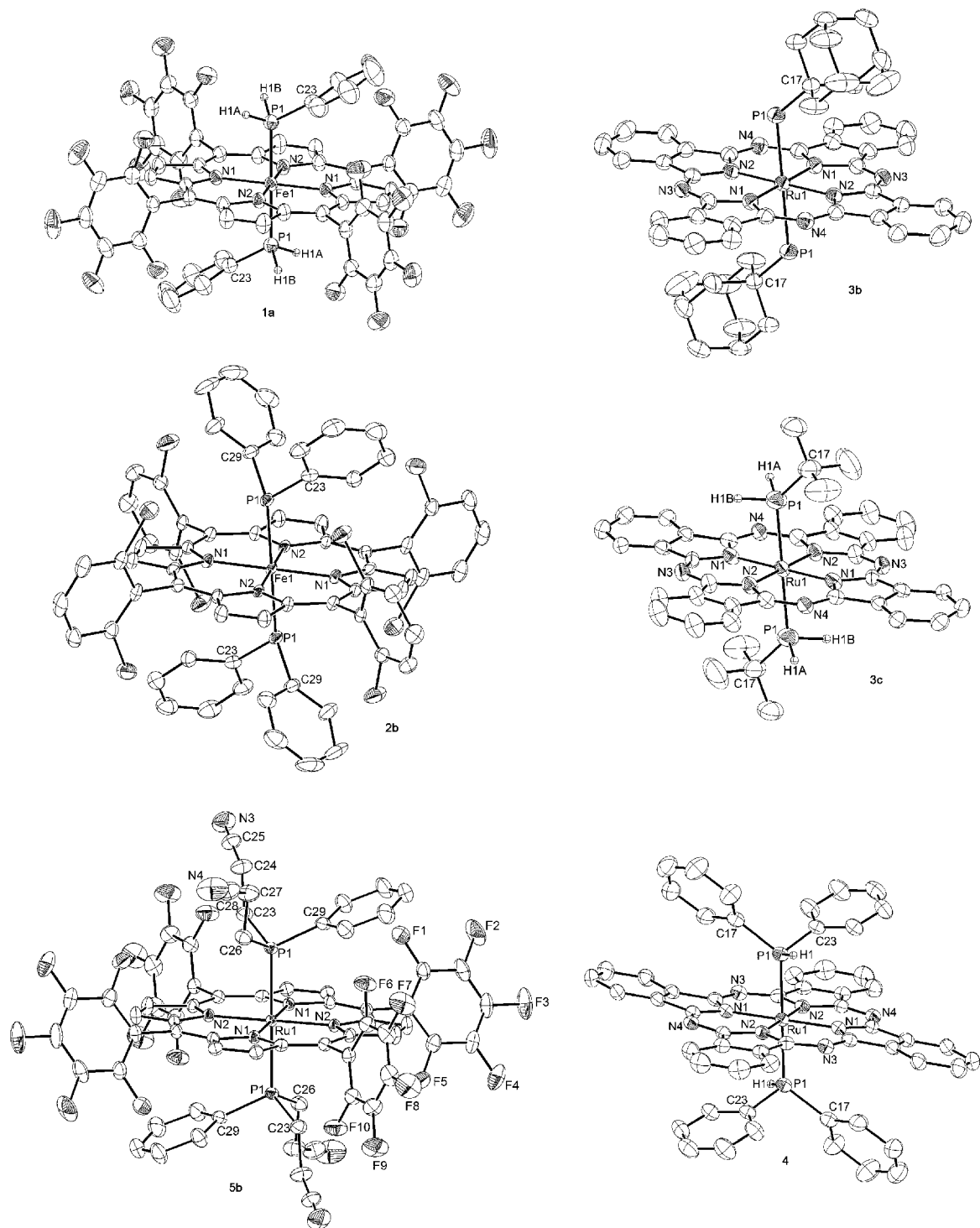


Figure 5. ORTEP drawings for **1a**, **2b**, **3b,c**, **4**, and **5b** with omission of the hydrogen atoms, except those bonded to P atoms (in **2b** and **3b**, the hydrogen atoms bonded to P atoms were not located). Thermal ellipsoid probability level: 30%. For **3c** and **4**, there are two independent molecules in the unit cell; only one molecule is shown.

purchased from Aldrich and were used as received. UV-vis spectra were recorded on a Hewlett-Packard 8453 diode array spectrophotometer (interfaced with an IBM-compatible PC). ^1H and ^{31}P NMR spectra were recorded on a Bruker DPX-300, AV-400, or DRX-500 spectrometer; the chemical shifts (δ , ppm) are relative to tetramethylsilane (TMS) for ^1H NMR and 85% H_3PO_4 for ^{31}P NMR. Fast atom bombardment (FAB) mass spectra were recorded on a Finnigan MAT 95 mass spectrometer

with 3-nitrobenzyl alcohol as the matrix. Elemental analyses were performed by the Institute of Chemistry, the Chinese Academy of Sciences.

Preparation of $[\text{Fe}^{\text{II}}(\text{Por})(\text{PH}_2\text{R})_2]$ and $[\text{Fe}^{\text{II}}(\text{Por})(\text{PHR})_2]$. A solution of $\text{Na}_2\text{S}_2\text{O}_4$ (100 mg) in water (5 mL) was mixed with a solution of $[\text{Fe}^{\text{III}}(\text{Por})\text{Cl}]$ (30 mg) in dichloromethane (15 mL) under nitrogen. The mixture was stirred for 15 min, resulting in a color change from dark red to bright red. Excess PH_2Ph or

Table 3. Average Values of M–P, M–N, and P–C Distances (Å) and M–P–C Angles (deg) for **1a**, **2b** (M = Fe), **3b,c**, **4**, and **5b** (M = Ru) as Compared with Those for the Previously Reported Iron(II) and Ruthenium(II) Porphyrin Analogues

complex	M–P	M–N	P–C	M–P–C
[Fe ^{II} (F ₂₀ -TPP)(PH ₂ Ph) ₂] (1a)	2.2597(9)	1.998(2)	1.803(4)	120.31(11)
[Fe ^{II} (2,6-Cl ₂ TPP)(PHPh ₂) ₂] (2b)	2.309(2)	1.999(5)	1.817(7)	123.1(2)
[Ru ^{II} (Pc)(PH ₂ Ad) ₂] (3b)	2.3707(13)	2.007(4)	1.844(5)	128.50(16)
[Ru ^{II} (Pc)(PH ₂ Bu ^u) ₂] (3c)	2.373(2)	2.002(4)	1.758(9)	133.6(4)
[Ru ^{II} (Pc)(PHPh ₂) ₂] (4)	2.3478(11)	2.016(2)	1.844(4)	120.33(12)
[Ru ^{II} (F ₂₀ -TPP)(PH ₂ Ph) ₂] ^{7a}	2.3603(10)	2.055(2)	1.824(3)	129.11(11)
[Ru ^{II} (F ₂₀ -TPP)(PH ₂ Mes) ₂] ^{7b}	2.358(20)	2.052(25)	1.811(18)	120.41(11)
[Ru ^{II} (TTP)(PH ₂ Ad) ₂]·2C ₅ H ₁₂ ^{7b}	2.349(26)	2.055(45)	1.844(21)	128.34(10)
[Ru ^{II} (F ₂₀ -TPP)(PHPh ₂) ₂] ^{7a}	2.3516(13)	2.055(3)	1.817(4)	121.17(12)
[Ru ^{II} (4-Cl-TPP)(PHPh ₂) ₂] ^{7a}	2.3397(11)	2.050(3)	1.814(4)	129.72(14)
[Ru ^{II} (F ₂₀ -TPP)(P(CH ₂ CH ₂ CN) ₂ Ph) ₂] (5b)	2.3754(10)	2.057(3)	1.834(5)	113.85(15)
[Fe ^{II} (TPP)(PMe ₂ Ph) ₂] ^{12j}	2.284(1)	2.000(1)	1.819(2)	115.97(9)
[Fe ^{II} (TPP)(PBu ⁿ) ₃] ₂ ^{12k}	2.3457(11)	1.996(3)	1.839(6)	115.76(15)
[Ru ^{II} (TPP)(PPh ₂ CH ₂ PPh ₂) ₂] ²¹	2.398(3)	2.042(8)	1.83(1)	115.7(4)
[Ru ^{II} (F ₂₀ -TPP)(PPh ₃) ₂] ²²	2.4643(9)	2.046(3)	1.850(3)	116.54(11)
[Ru ^{II} (F ₂₈ -TPP)(PPh ₃) ₂] ²²	2.4807(7)	2.0497(18)	1.839(3)	115.95(9)

PHPh₂ (neat liquid, two drops) or PH₂Ad (4 equiv) was then added. Upon stirring for 5 min, the organic phase was separated from the aqueous one, dried with anhydrous Na₂SO₄, and evaporated to dryness in vacuo. The crude product (dark red solid) was purified by washing with hexane.

[Fe^{II}(F₂₀-TPP)(PH₂Ph)₂] (1a). Yield: 56%. ¹H NMR (400 MHz, CDCl₃, –25 °C): δ H_β 8.34 (s, 8H); H_p 6.65 (m, 2H); H_m 6.29 (m, 4H); H_o 4.16 (m, 4H); PH₂ –0.39 (s), –0.46 (s), –0.59 (br), –0.82 (br), –0.94 (s), –1.02 (s) (a total of 4H). ³¹P{¹H} NMR (162 MHz, CDCl₃, –25 °C): δ –34.8. UV–vis (CH₂Cl₂ containing 2 × 10^{–2} M of PH₂Ph): λ_{max} 415 sh, 448 (Soret), 546 nm. FAB MS: *m/z* 1248 (M⁺), 1138 ([M – PH₂Ph]⁺), 1028 ([M – 2PH₂Ph]⁺). Anal. calcd for C₅₆H₂₂F₂₀FeN₄P₂: C, 53.87; H, 1.78; N, 4.49. Found: C, 54.11; H, 1.90; N, 4.34.

[Fe^{II}(F₂₀-TPP)(PH₂Ad)₂] (1b). Yield: 64%. ¹H NMR (500 MHz, CDCl₃, –25 °C): δ H_β 8.38 (s, 8H); Ad 0.83 (s, 12H), 0.54 (m, 6H), –1.31 (s, 12H); PH₂ –1.98 (s), –2.10 (s), –2.21 (br), –2.50 (br), –2.62 (s), –2.74 (s) (a total of 4H). ³¹P{¹H} NMR (162 MHz, CDCl₃, –25 °C): δ –8.7. UV–vis (CH₂Cl₂ containing 2 × 10^{–2} M of PH₂Ad): λ_{max} 410 sh, 451 (Soret), 551 nm. FAB MS: *m/z* 1364 (M⁺), 1196 ([M – PH₂Ad]⁺), 1028 ([M – 2PH₂Ad]⁺). Anal. calcd for C₆₄H₄₂F₂₀FeN₄P₂: C, 56.32; H, 3.10; N, 4.11. Found: C, 56.68; H, 2.94; N, 3.88.

[Fe^{II}(F₂₀-TPP)(PHPh₂)₂] (2a). Yield: 60%. ¹H NMR (400 MHz, CDCl₃): δ H_β 8.25 (s, 8H); H_p 6.71 (m, 4H); H_m 6.38 (m, 8H); H_o 4.35 (m, 8H); PH 0.35 (s), 0.10 (br), –0.24 (br), –0.49 (s) (a total of 2H). ³¹P{¹H} NMR (162 MHz, CDCl₃): δ 21.7. UV–vis (CH₂Cl₂ containing 2 × 10^{–2} M of PHPh₂): λ_{max} 454 (Soret), 550 nm. FAB MS: *m/z* 1401 ([M + H]⁺), 1214 ([M – PHPh₂]⁺), 1028 ([M – 2PHPh₂]⁺). Anal. calcd for C₆₈H₃₀F₂₀FeN₄P₂: C, 58.31; H, 2.16; N, 4.00. Found: C, 58.68; H, 2.28; N, 3.84.

[Fe^{II}(2,6-Cl₂TPP)(PHPh₂)₂] (2b). Yield: 61%. ¹H NMR (500 MHz, CDCl₃, –25 °C): δ H_β 8.28 (s, 8H); H'_m 7.62 (m, 8H); H'_p 7.53 (m, 4H); H_p 6.58 (m, 4H); H_m 6.31 (m, 8H); H_o 4.68 (m, 8H); PH 0.67 (s), 0.47 (br), 0.18 (br), –0.02 (s) (a total of 2H). (H'_m and H'_p are the phenyl signals of the 2,6-Cl₂TPP ligand). ³¹P{¹H} NMR (202 MHz, CDCl₃, –25 °C): δ 21.0. UV–vis (CH₂Cl₂ containing 2 × 10^{–2} M of PHPh₂): λ_{max} 454 (Soret), 552 nm. FAB MS: *m/z* 1316 (M⁺), 1130 ([M – PHPh₂]⁺), 944 ([M – 2PHPh₂]⁺). Anal. calcd for C₆₈H₄₂Cl₈FeN₄P₂·H₂O: C, 61.20; H, 3.32; N, 4.20. Found: C, 61.52; H, 3.46; N, 4.00.

Preparation of [Ru^{II}(Pc)(PH₂Ph)₂] and [Ru^{II}(Pc)(PHPh₂)₂]. Phenylphosphine or diphenylphosphine (10 wt % in hexane, 10 mL) was added to a solution of [Ru^{II}(Pc)(DMSO)₂] (500 mg, 0.65 mmol) in dichloromethane (20 mL). The mixture was stirred overnight and then treated with hexane (50 mL), leading to the

formation of a dark blue-purple precipitate. The precipitate was collected by filtration and washed with hexane until the filtrate became colorless.

[Ru^{II}(Pc)(PH₂Ph)₂] (3a). Yield: 65%. ¹H NMR (400 MHz, CDCl₃): δ Pc 9.11 (m, 8H), 7.91 (m, 8H); H_p 6.65 (m, 2H); H_m 6.23 (m, 4H); H_o 4.32 (m, 4H); PH₂ 0.17 (s), 0.03 (br) –0.13 (br), –0.37 (br), –0.53 (s), –0.67 (s) ppm (a total of 4H). ³¹P{¹H} NMR (162 MHz, CDCl₃): δ –57.2. UV–vis (1.3 × 10^{–5} M, CH₂Cl₂): λ_{max} (log ε) 315 (4.8), 402 (3.9) sh, 582 (4.3) sh, 640 (4.8) nm. FAB MS: *m/z* 834 (M⁺), 724 ([M – PH₂Ph]⁺), 614 ([M – 2PH₂Ph]⁺). Anal. calcd for C₄₄H₃₀N₈P₂Ru·CH₂Cl₂: C, 58.83; H, 3.51; N, 12.20. Found: C, 58.82; H, 3.51; N, 12.42.

[Ru^{II}(Pc)(PHPh₂)₂] (4). Yield: 60%. ¹H NMR (400 MHz, CDCl₃): δ Pc 9.03 (m, 8H), 7.87 (m, 8H); H_p 6.63 (m, 4H); H_m 6.24 (m, 8H); H_o 4.43 (m, 8H); PH 0.80 (s), 0.51 (br), 0.23 (br), –0.05 (s) (a total of 2H). ³¹P{¹H} NMR (162 MHz, CDCl₃): δ 3.7. UV–vis (1.4 × 10^{–5} M, CH₂Cl₂): λ_{max} (log ε) 291 (4.8), 410 (4.0) sh, 580 (4.3) sh, 640 (4.8) nm. FAB MS: *m/z* 986 (M⁺), 800 ([M – PHPh₂]⁺), 614 ([M – 2PHPh₂]⁺). Anal. calcd for C₅₆H₃₈N₈P₂Ru·CH₂Cl₂: C, 63.93; H, 3.76; N, 10.46. Found: C, 64.07; H, 3.85; N, 10.57.

Preparation of [Ru^{II}(Pc)(PH₂R)₂] (R = Ad, 3b; Bu^u, 3c). LiAlH₄ (500 mg) was added to a mixture of [Ru^{II}(Pc)(DMSO)₂] (500 mg, 0.65 mmol) and O=PcAd (658 mg, 2.6 mmol, for **3b**) or PcBu^u (413 mg, 2.6 mmol, for **3c**) in dichloromethane. The mixture was stirred overnight and subsequently treated with methanol until no H₂ bubbles evolved. After filtration, the filtrate was evaporated to dryness to give a dark blue-purple solid. The solid was collected, washed with methanol, and recrystallized from dichloromethane–hexane.

[Ru^{II}(Pc)(PH₂Ad)₂] (3b). Yield: 70%. ¹H NMR (400 MHz, CDCl₃): δ Pc 9.22 (m, 8H), 7.94 (m, 8H); Ad 0.86 (m, 12H), 0.44 (m, 6H), –1.14 (s, 12H); PH₂ –1.38 (s), –1.50 (s), –1.66 (br), –1.90 (br), –2.05 (s), –2.17 (s) (a total of 4H). ³¹P{¹H} NMR (162 MHz, CDCl₃): δ –23.4. UV–vis (1.1 × 10^{–5} M, CH₂Cl₂): λ_{max} (log ε) 316 (4.8), 403 (3.9) sh, 578 (4.3) sh, 637 (4.8). FAB MS: *m/z* 950 (M⁺), 782 ([M – PH₂Ad]⁺), 614 ([M – 2PH₂Ad]⁺). Anal. calcd for C₅₂H₅₀N₈P₂Ru·CH₂Cl₂: C, 61.51; H, 5.06; N, 10.83. Found: C, 61.71; H, 4.94; N, 11.02.

[Ru^{II}(Pc)(PH₂Bu^u)₂] (3c). Yield: 70%. ¹H NMR (300 MHz, CDCl₃): δ Pc 9.23 (m, 8H), 7.96 (m, 8H); Bu^u and PH₂ –1.28 (m, 19H), –1.02 (s), –1.70 (br), –1.91 (br), –2.07 (s) (a total of 3H). ³¹P{¹H} NMR (162 MHz, CDCl₃): δ –18.2. UV–vis (1.8 × 10^{–5} M, CH₂Cl₂): λ_{max} (log ε) 316 (4.4), 403 (3.4) sh, 579 (3.8) sh, 638 (4.4). FAB MS: *m/z* 794 (M⁺), 704 ([M – PH₂Bu^u]⁺), 614 ([M –

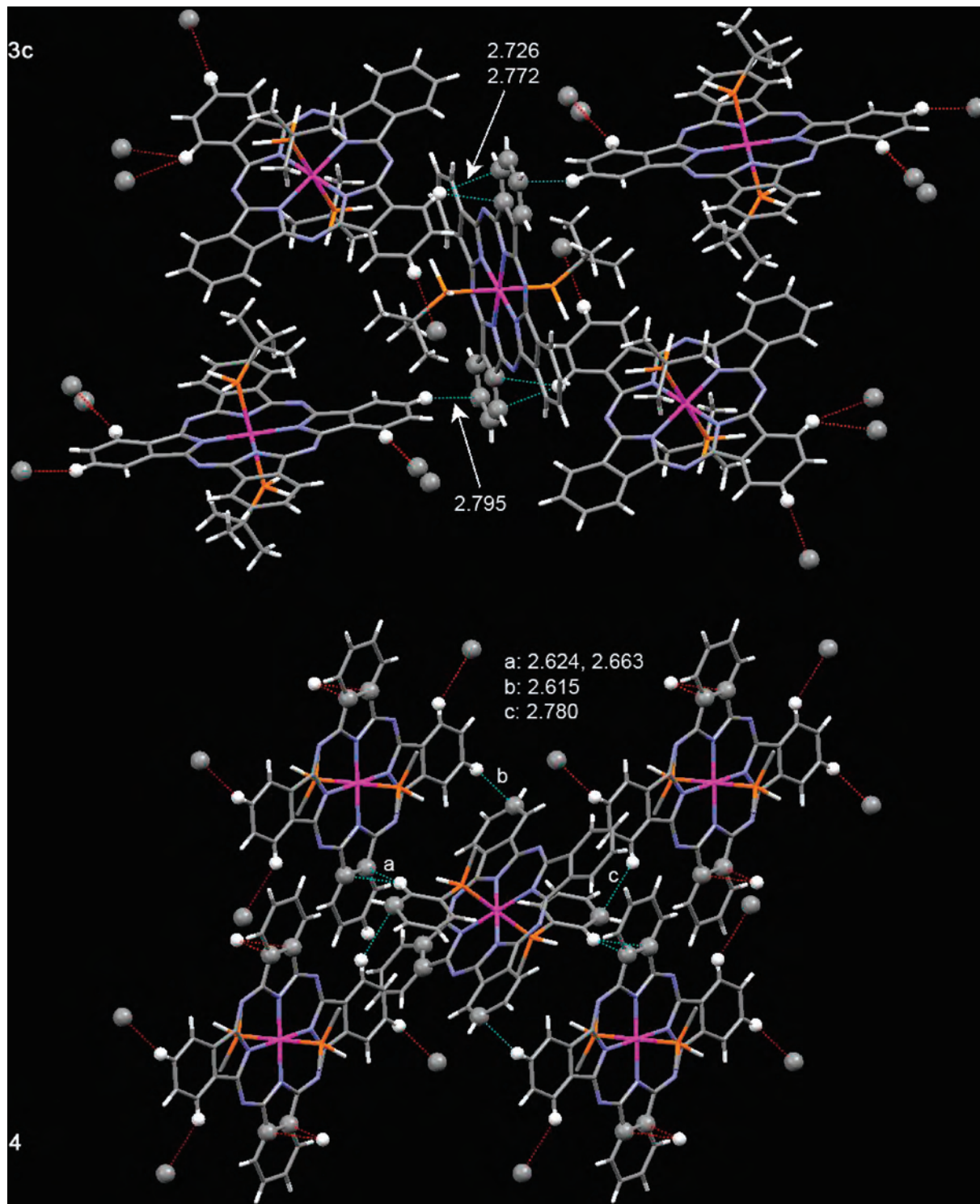


Figure 6. C–H··· π interactions in the crystal structures of **3c** and **4**. For **4**, the $\text{P}(\text{HPh}_2)$ phenyl groups not involved in the C–H··· π interactions are not shown, except for their C atoms bonded to the P atoms.

$2\text{PH}_2\text{Bu}^{\text{I}^+}$). Anal. calcd for $\text{C}_{40}\text{H}_{38}\text{N}_8\text{P}_2\text{Ru}\cdot\text{CH}_2\text{Cl}_2\cdot\text{H}_2\text{O}$: C, 54.91; H, 4.72; N, 12.49. Found: C, 54.89; H, 4.70; N, 12.36.

Reaction of $[\text{Ru}^{\text{II}}(\text{F}_{20}\text{-TPP})(\text{PH}_2\text{Ph})_2]$ or $[\text{Ru}^{\text{II}}(\text{F}_{20}\text{-TPP})(\text{PHPh}_2)_2]$ with Alkenes $\text{CH}_2=\text{CHR}$ ($\text{R} = \text{CO}_2\text{Et}$, CN) and Isolation of $[\text{Ru}^{\text{II}}(\text{F}_{20}\text{-TPP})(\text{P}(\text{CH}_2\text{CH}_2\text{R})_2\text{Ph})_2]$ (5**) or $[\text{Ru}^{\text{II}}(\text{F}_{20}\text{-TPP})(\text{P}(\text{CH}_2\text{CH}_2\text{R})_2\text{Ph})_2]$ (**6**).** $[\text{Ru}^{\text{II}}(\text{F}_{20}\text{-TPP})(\text{PH}_2\text{Ph})_2]$ or $[\text{Ru}^{\text{II}}(\text{F}_{20}\text{-TPP})(\text{PHPh}_2)_2]$ (0.01 mmol) was dissolved in acetone (20 mL) and then degassed for 5 min. To this solution was added $\text{CH}_2=\text{CHCO}_2\text{Et}$ or $\text{CH}_2=\text{CHCN}$ (0.04 mmol for $[\text{Ru}^{\text{II}}(\text{F}_{20}\text{-TPP})(\text{PH}_2\text{Ph})_2]$, 0.02 mmol for $[\text{Ru}^{\text{II}}(\text{F}_{20}\text{-TPP})(\text{PHPh}_2)_2]$) and $t\text{-BuOK}$

(4.4 mg, 0.04 mmol). The color of the solution changed from red to red-brown immediately. The mixture was stirred for 10 min and then evaporated in vacuo to a volume of 1 mL. The addition of diethyl ether (10 mL) led to the precipitation of **5** or **6** as a red-purple solid, which was collected by filtration, washed with three portions of diethyl ether (3×5 mL), and dried in vacuo.

$[\text{Ru}^{\text{II}}(\text{F}_{20}\text{-TPP})(\text{P}(\text{CH}_2\text{CH}_2\text{CO}_2\text{Et})_2\text{Ph})_2]$ (5a**).** Yield: 85%. ^1H NMR (300 MHz, CDCl_3): δ H_β 8.14 (s, 8H); H_p 6.75 (m, 2H); H_m 6.50 (m, 4H); H_o 4.39 (m, 4H); Et 3.75 (m, 8H), 0.99 (t, $J = 6.5$ Hz, 12 H); H_c , H_d -0.04 (m, 4H), -0.18 (m, 4H); H_a , H_b -1.44 (m, 4H),

-1.98 (m, 4H). $^{31}\text{P}\{^1\text{H}\}$ NMR (400 MHz, CDCl_3): δ 8.1. UV-vis (CH_2Cl_2): λ_{max} 419 sh, 439 (Soret), 524 nm. FAB MS: m/z 1695 ($[\text{M} + \text{H}]^+$), 1384 ($[\text{M} - \text{P}(\text{CH}_2\text{CH}_2\text{CO}_2\text{Et})_2\text{Ph}]^+$), 1074 ($[\text{M} - 2\text{P}(\text{CH}_2\text{CH}_2\text{CO}_2\text{Et})_2\text{Ph}]^+$). Anal. calcd for $\text{C}_7\text{H}_5\text{F}_{20}\text{N}_4\text{O}_8\text{P}_2\text{Ru}$: C, 53.88; H, 3.21; N, 3.31. Found: C, 54.31; H, 3.40; N, 3.48.

[Ru^{II}(F₂₀-TPP)(P(CH₂CH₂CN)₂Ph)₂] (5b). Yield: 87%. ^1H NMR (400 MHz, $(\text{CD}_3)_2\text{CO}$): δ H _{β} 8.60 (s, 8H); H _{p} 6.94 (m, 2H); H _{m} 6.67 (m, 4H); H _{o} 4.43 (m, 4H); H _{c} , H _{d} 0.23 (m, 4H), 0.06 (m, 4H); H _{a} , H _{b} -1.34 (m, 4H), -1.83 (m, 4H). $^{31}\text{P}\{^1\text{H}\}$ NMR (400 MHz, $(\text{CD}_3)_2\text{CO}$): δ 8.3 ppm. UV-vis (CH_2Cl_2): λ_{max} 413 sh, 433 (Soret), 518 nm. FAB MS: m/z 1507 ($[\text{M} + \text{H}]^+$), 1290 ($[\text{M} - \text{P}(\text{CH}_2\text{CH}_2\text{CN})_2\text{Ph}]^+$), 1074 ($[\text{M} - 2\text{P}(\text{CH}_2\text{CH}_2\text{CN})_2\text{Ph}]^+$). Anal. calcd for $\text{C}_6\text{H}_3\text{F}_{20}\text{N}_8\text{P}_2\text{Ru}$: C, 54.23; H, 2.28; N, 7.44. Found: C, 53.91; H, 2.43; N, 7.62.

[Ru^{II}(F₂₀-TPP)(P(CH₂CH₂CO₂Et)Ph)₂] (6a). Yield: 80%. ^1H NMR (300 MHz, CD_3Cl): δ H _{β} 8.09 (s, 8H); H _{p} 6.77 (m, 4H); H _{m} 6.49 (m, 8H); H _{o} 4.33 (m, 8H); Et 3.63 (q, $J = 7.1$ Hz, 4H), 0.92 (t, $J = 7.1$ Hz, 6H); H _{b} -0.25 (m, 4H); H _{a} -1.71 (m, 4H). $^{31}\text{P}\{^1\text{H}\}$ NMR (400 MHz, $(\text{CD}_3)_2\text{CO}$): δ 9.9. UV-vis (CH_2Cl_2): λ_{max} 421 sh, 439 (Soret), 524 nm. FAB MS: m/z 1647 ($[\text{M} + \text{H}]^+$), 1360 ($[\text{M} - \text{P}(\text{CH}_2\text{CH}_2\text{CO}_2\text{Et})\text{Ph}]^+$), 1074 ($[\text{M} - 2\text{P}(\text{CH}_2\text{CH}_2\text{CO}_2\text{Et})\text{Ph}]^+$). Anal. calcd for $\text{C}_7\text{H}_4\text{F}_{20}\text{N}_4\text{O}_4\text{P}_2\text{Ru}$: C, 56.91; H, 2.82; N, 3.40. Found: C, 56.81; H, 2.97; N, 3.18.

[Ru^{II}(F₂₀-TPP)(P(CH₂CH₂CN)Ph)₂] (6b). Yield: 82%. ^1H NMR (400 MHz, $(\text{CD}_3)_2\text{CO}$): δ H _{β} 8.42 (s, 8H); H _{p} 6.87 (m, 4H); H _{m} 6.57 (m, 8H); H _{o} 4.34 (m, 8H); H _{b} -0.25 (m, 4H); H _{a} -1.66 (m, 4H). $^{31}\text{P}\{^1\text{H}\}$ NMR (400 MHz, $(\text{CD}_3)_2\text{CO}$): δ 9.6. UV-vis (CH_2Cl_2): λ_{max} 412 sh, 438 (Soret), 520 nm. FAB MS: m/z 1553 ($[\text{M} + \text{H}]^+$), 1313 ($[\text{M} - \text{P}(\text{CH}_2\text{CH}_2\text{CN})\text{Ph}]^+$), 1074 ($[\text{M} - 2\text{P}(\text{CH}_2\text{CH}_2\text{CN})\text{Ph}]^+$). Anal. calcd for $\text{C}_7\text{H}_3\text{F}_{20}\text{N}_6\text{P}_2\text{Ru} \cdot \text{H}_2\text{O}$: C, 56.61; H, 2.44; N, 5.35. Found: C, 56.24; H, 2.41; N, 5.19.

Reaction of [Ru^{II}(Pc)(PH₂Ph)₂] or [Ru^{II}(Pc)(PHPh)₂] with Alkenes CH(R¹)=CR²R³ (R¹ = R² = H, R³ = CO₂Et, CN, C(O)Me, P(O)(OEt)₂, S(O)₂Ph; R¹ = H, R² = Me, R³ = CO₂Me; R¹ = R³ = CO₂Me, R² = H) and Isolation of [Ru^{II}(Pc)(P(CH₂-CH₂CN)₂Ph)₂] (7) or [Ru^{II}(Pc)(P(CH(R¹)CHR²R³)Ph)₂] (9). To a solution of [Ru^{II}(Pc)(PH₂Ph)₂] or [Ru^{II}(Pc)(PHPh)₂] (40 mg) in THF (6 mL) was added CH(R¹)=CR²R³ (20 mg for the alkene with R¹ = R² = H, R³ = S(O)₂Ph; 20 μL for the other alkenes) and ^tBuOK (20 mg). The mixture was stirred for 1 h, followed by removal of the solvent in vacuo. The residue was dissolved in dichloromethane. Upon filtration, the filtrate was evaporated in vacuo to dryness, and the residual dark blue-purple solid was recrystallized from dichloromethane-cyclohexane.

[Ru^{II}(Pc)(P(CH₂CH₂CN)₂Ph)₂] (7). Yield: 60%. ^1H NMR (300 MHz, CDCl_3): δ Pc 9.10 (m, 8H), 7.98 (m, 8H); H _{p} 6.84 (m, 2H); H _{m} 6.40 (m, 4H); H _{o} 4.24 (m, 4H); H _{c} , H _{d} 0.16 (m, 4H), -0.02 (m, 4H); H _{a} , H _{b} -1.21 (m, 4H), -1.71 (m, 4H). $^{31}\text{P}\{^1\text{H}\}$ NMR (162 MHz, CDCl_3): δ 11.0. UV-vis (5.5×10^{-5} M, CH_2Cl_2): λ_{max} (log ϵ) 315 (4.4), 438 (3.3) sh, 581 (3.9) sh, 640 (4.3) nm. FAB MS: m/z 1046 (M^+), 830 ($[\text{M} - \text{P}(\text{CH}_2\text{CH}_2\text{CN})_2\text{Ph}]^+$), 614 ($[\text{M} - 2\text{P}(\text{CH}_2\text{CH}_2\text{CN})_2\text{Ph}]^+$). Anal. calcd for $\text{C}_5\text{H}_4\text{N}_{12}\text{P}_2\text{Ru} \cdot \text{CH}_2\text{Cl}_2$: C, 60.53; H, 3.92; N, 14.86. Found: C, 60.58; H, 3.99; N, 14.98.

[Ru^{II}(Pc)(P(CH₂CH₂CO₂Et)Ph)₂] (9a). Yield: 68%. ^1H NMR (300 MHz, CDCl_3): δ Pc 9.01 (m, 8H), 7.85 (m, 8H); H _{p} 6.71 (m, 4H); H _{m} 6.29 (m, 8H); H _{o} 4.40 (m, 8H); Et 3.46 (q, $J = 6.5$ Hz, 4H), 0.81 (t, $J = 6.1$ Hz, 6H); H _{b} -0.22 (m, 4H); H _{a} -1.51 (m, 4H). $^{31}\text{P}\{^1\text{H}\}$ NMR (202 MHz, CDCl_3): δ 10.5. UV-vis ($7.8 \times$

10^{-5} M, CH_2Cl_2): λ_{max} (log ϵ) 297 (4.3), 418 (3.4) sh, 581 (3.8) sh, 639 (4.2) nm. FAB MS: m/z 1186 (M^+), 900 ($[\text{M} - \text{P}(\text{CH}_2\text{CH}_2\text{CO}_2\text{Et})\text{Ph}]^+$), 614 ($[\text{M} - 2\text{P}(\text{CH}_2\text{CH}_2\text{CO}_2\text{Et})\text{Ph}]^+$). Anal. calcd for $\text{C}_6\text{H}_5\text{N}_8\text{O}_4\text{P}_2\text{Ru} \cdot \text{CH}_2\text{Cl}_2$: C, 63.31; H, 4.44; N, 8.82. Found: C, 63.04; H, 4.32; N, 8.84.

[Ru^{II}(Pc)(P(CH₂CH₂CN)Ph)₂] (9b). Yield: 74%. ^1H NMR (300 MHz, CDCl_3): δ Pc 9.03 (m, 8H), 7.91 (m, 8H); H _{p} 6.78 (m, 4H); H _{m} 6.35 (m, 8H); H _{o} 4.37 (m, 8H); H _{b} -0.20 (m, 4H); H _{a} -1.56 (m, 4H). $^{31}\text{P}\{^1\text{H}\}$ NMR (162 MHz, CDCl_3): δ 10.3. UV-vis (1.1×10^{-5} M, CH_2Cl_2): λ_{max} (log ϵ) 296 (4.6), 418 (3.5) sh, 582 (4.1) sh, 641 (4.5) nm. FAB MS: m/z 1092 (M^+), 853 ($[\text{M} - \text{P}(\text{CH}_2\text{CH}_2\text{CN})\text{Ph}]^+$), 614 ($[\text{M} - 2\text{P}(\text{CH}_2\text{CH}_2\text{CN})\text{Ph}]^+$). Anal. calcd for $\text{C}_6\text{H}_4\text{N}_{10}\text{P}_2\text{Ru} \cdot 2\text{CH}_2\text{Cl}_2$: C, 60.91; H, 3.83; N, 11.10. Found: C, 61.09; H, 4.00; N, 10.95.

[Ru^{II}(Pc)(P(CH₂CH₂C(O)Me)Ph)₂] (9c). Yield: 66%. ^1H NMR (300 MHz, CDCl_3): δ Pc 9.01 (m, 8H), 7.87 (m, 8H); H _{p} 6.73 (m, 4H); H _{m} 6.30 (m, 8H); H _{o} 4.40 (m, 8H); Me 1.05 (s, 6H); H _{b} -0.29 (m, 4H); H _{a} -1.41 (m, 4H). $^{31}\text{P}\{^1\text{H}\}$ NMR (162 MHz, CDCl_3): δ 8.3. UV-vis (1.5×10^{-5} M, CH_2Cl_2): λ_{max} (log ϵ) 296 (4.6), 419 (3.6) sh, 578 (4.1) sh, 638 (4.5) nm. FAB MS: m/z 1126 (M^+), 870 ($[\text{M} - \text{P}(\text{CH}_2\text{CH}_2\text{C(O)Me})\text{Ph}]^+$), 614 ($[\text{M} - 2\text{P}(\text{CH}_2\text{CH}_2\text{C(O)Me})\text{Ph}]^+$). Anal. calcd for $\text{C}_6\text{H}_5\text{N}_8\text{O}_2\text{P}_2\text{Ru} \cdot 2\text{CH}_2\text{Cl}_2$: C, 61.16; H, 4.20; N, 8.65. Found: C, 60.85; H, 4.24; N, 8.65.

[Ru^{II}(Pc)(P(CH₂CH₂P(O)(OEt)₂)Ph)₂] (9d). Yield: 63%. ^1H NMR (300 MHz, CDCl_3): δ Pc 8.99 (m, 8H), 7.85 (m, 8H); H _{p} 6.74 (m, 4H); H _{m} 6.34 (m, 8H); H _{o} 4.39 (m, 8H); Et 3.45 (m, 8H), 0.96 (m, 12H); H _{b} -0.77 (m, 4H); H _{a} -1.74 (m, 4H). $^{31}\text{P}\{^1\text{H}\}$ NMR (162 MHz, CDCl_3): δ 29.4 (t), 14.3 (t). UV-vis (8.3×10^{-5} M, CH_2Cl_2): λ_{max} (log ϵ) 298 (4.4), 418 (3.7) sh, 582 (4.2) sh, 637 (4.4) nm. FAB MS: m/z 1314 (M^+), 964 ($[\text{M} - \text{P}(\text{CH}_2\text{CH}_2\text{P(O)(OEt)₂)Ph}]^+$), 614 ($[\text{M} - 2\text{P}(\text{CH}_2\text{CH}_2\text{P(O)(OEt)₂)Ph}]^+$). Anal. calcd for $\text{C}_6\text{H}_6\text{N}_8\text{O}_6\text{P}_4\text{Ru} \cdot \text{CH}_2\text{Cl}_2$: C, 59.23; H, 4.75; N, 8.01. Found: C, 59.39; H, 4.72; N, 8.23.

[Ru^{II}(Pc)(P(CH₂CH₂S(O)₂Ph)Ph)₂] (9e). Yield: 76%. ^1H NMR (300 MHz, CDCl_3): δ Pc 9.00 (m, 8H), 7.91 (m, 8H); S(O)₂Ph 7.60 (m, 4H), 7.31 (m, 2H), 6.96 (m, 4H); H _{p} 6.69 (m, 4H); H _{m} 6.21 (m, 8H); H _{o} 4.11 (m, 8H); H _{b} 0.52 (m, 4H); H _{a} -1.77 (m, 4H). $^{31}\text{P}\{^1\text{H}\}$ NMR (162 MHz, CDCl_3): δ 11.1. UV-vis (3.0×10^{-5} M, CH_2Cl_2): λ_{max} (log ϵ) 295 (4.4), 418 (3.4) sh, 580 (3.8) sh, 641 (4.3) nm. FAB MS: m/z 1322 (M^+), 968 ($[\text{M} - \text{P}(\text{CH}_2\text{CH}_2\text{S(O)₂Ph})\text{Ph}]^+$), 614 ($[\text{M} - 2\text{P}(\text{CH}_2\text{CH}_2\text{S(O)₂Ph})\text{Ph}]^+$). Anal. calcd for $\text{C}_7\text{H}_5\text{N}_8\text{O}_4\text{P}_2\text{S}_2\text{Ru} \cdot 3\text{CH}_2\text{Cl}_2$: C, 57.11; H, 3.83; N, 7.10. Found: C, 57.48; H, 4.05; N, 6.90.

[Ru^{II}(Pc)(P(CH₂CH(Me)CO₂Me)Ph)₂] (9f). Yield: 56%. ^1H NMR (300 MHz, CDCl_3): δ Pc 9.00 (m, 8H), 7.85 (m, 8H); H _{p} 6.70 (m, 4H); H _{m} 6.25 (m, 8H); H _{o} 4.40 (m, 8H); Me' 2.46 (s, 6H); H _{c} -0.04 (br, 2H); Me -0.31 (m, 6H); H _{a} , H _{b} -1.08 (m, 2H), -2.02 (m, 2H). $^{31}\text{P}\{^1\text{H}\}$ NMR (162 MHz, CDCl_3): δ 10.6. UV-vis (7.3×10^{-5} M, CH_2Cl_2): λ_{max} (log ϵ) 302 (4.5), 418 (3.8) sh, 582 (4.3) sh, 637 (4.6) nm. FAB MS: m/z 1186 (M^+), 900 ($[\text{M} - \text{P}(\text{CH}_2\text{CH}(\text{Me})\text{CO}_2\text{Me})\text{Ph}]^+$), 614 ($[\text{M} - 2\text{P}(\text{CH}_2\text{CH}(\text{Me})\text{CO}_2\text{Me})\text{Ph}]^+$). Anal. calcd for $\text{C}_6\text{H}_5\text{N}_8\text{O}_4\text{P}_2\text{Ru} \cdot \text{CH}_2\text{Cl}_2$: C, 63.31; H, 4.44; N, 8.82. Found: C, 63.27; H, 4.18; N, 8.74.

[Ru^{II}(Pc)(P(CH(CO₂Me)CH₂CO₂Me)Ph)₂] (9g). Yield: 72%. ^1H NMR (300 MHz, CDCl_3): δ Pc 9.00 (m, 8H), 7.89 (m, 8H); H _{p} 6.95 (m, 2H), 6.67 (m, 2H); H _{m} 6.27 (m, 4H), 6.17 (m, 4H); H _{o} 4.63 (m, 4H), 4.35 (m, 4H); Me 3.06 (m, 6H), 2.50 (s, 6H); H _{b} , H _{c} -0.28 (m, 2H), -0.40 (m, 2H); H _{a} -1.05 (br, 2H). (The multiplet at δ 3.06 became a singlet upon raising the temperature to 60 °C.) $^{31}\text{P}\{^1\text{H}\}$ NMR (162 MHz, CDCl_3): δ 9.1. UV-vis (1.4×10^{-5} M, CH_2Cl_2): λ_{max} (log ϵ) 299 (4.7), 416 (3.7) sh, 581 (4.3) sh, 643 (4.7) nm. FAB MS: m/z 1274 (M^+), 944 ($[\text{M} - \text{P}(\text{CH}(\text{CO}_2\text{Me})\text{CH}_2\text{CO}_2\text{Me})\text{Ph}]^+$), 614 ($[\text{M} - 2\text{P}(\text{CH}(\text{CO}_2\text{Me})\text{CH}_2\text{CO}_2\text{Me})\text{Ph}]^+$), 614 ($[\text{M} - 2\text{P}(\text{CH}(\text{CO}_2\text{Me})\text{CH}_2\text{CO}_2\text{Me})\text{Ph}]^+$), 614 ($[\text{M} - 2\text{P}(\text{CH}(\text{CO}_2\text{Me})\text{CH}_2\text{CO}_2\text{Me})\text{Ph}]^+$).

(24) Otwinowski, Z.; Minor, W. In *Methods in Enzymology*; Carter, C. W., Jr., Sweet, R. M., Eds.; Academic Press: New York, 1997; Vol. 276: Macromolecular Crystallography, Part A, p 307.

(25) Altomare, A.; Burla, M. C.; Camalli, M.; Cascarano, G. L.; Giacovazzo, C.; Guagliardi, A.; Moliterni, A. G. G.; Polidori, G.; Spagna, R. *J. Appl. Crystallogr.* **1999**, *32*, 115.

CO₂Me)Ph₂)⁺). Anal. calcd for C₆₈H₅₄N₈O₈P₂Ru·1.5CH₂Cl₂: C, 59.56; H, 4.10; N, 7.99. Found: C, 59.36; H, 4.43; N, 7.60.

Reaction of [Ru^{II}(Pc)(PH₂Ph)₂] or [Ru^{II}(Pc)(PMPH₂)₂] with RX (X = I, R = Me; X = Br, R = Buⁿ, CH₂=CHCH₂, MeC≡CCH₂, HC≡CCH₂; X = Cl, R = Bn) and Isolation of [Ru^{II}(Pc)(PMe₂Ph)₂] (8) or [Ru^{II}(Pc)(PRPh₂)₂] (10). The procedure is similar to that for the reaction of [Ru^{II}(Pc)(PH₂Ph)₂] or [Ru^{II}(Pc)(PMPH₂)₂] with alkenes CH(R¹)=CR²R³, except that halo compounds RX (20 μL), instead of alkenes, were used.

[Ru^{II}(Pc)(PMe₂Ph)₂] (8). Yield: 49%. ¹H NMR (300 MHz, CDCl₃): δ Pc 9.05 (m, 8H), 7.86 (m, 8H); H_p 6.63 (m, 2H); H_m 6.28 (m, 4H); H_o 4.35 (m, 4H); Me -2.09 (s, 12H). ³¹P{¹H} NMR (162 MHz, CDCl₃): δ -1.3. UV-vis (3.7 × 10⁻⁵ M, CH₂Cl₂): λ_{max} (log ε) 306 (4.4), 428 (3.4) sh, 580 (3.8) sh, 634 (4.3) nm. FAB MS: *m/z* 890 (M⁺), 752 ([M - PMe₂Ph]⁺), 614 ([M - 2PMe₂Ph]⁺). Anal. calcd for C₄₈H₃₈N₈P₂Ru·0.5CH₂Cl₂: C, 62.48; H, 4.22; N, 12.02. Found: C, 62.68; H, 4.30; N, 11.96.

[Ru^{II}(Pc)(PMePh₂)₂] (10a). Yield: 87%. ¹H NMR (400 MHz, CDCl₃): δ Pc 9.00 (m, 8H), 7.85 (m, 8H); H_p 6.66 (m, 4H); H_m 6.29 (m, 8H); H_o 4.44 (m, 8H); Me -1.84 (s, 6H). ³¹P{¹H} NMR (162 MHz, CDCl₃): δ -0.5. UV-vis (2.1 × 10⁻⁵ M, CH₂Cl₂): λ_{max} (log ε) 296 (4.5), 420 (3.5) sh, 579 (4.0) sh, 637 nm (4.4). FAB MS: *m/z* 1014 (M⁺), 814 ([M - PMePh₂]⁺), 614 ([M - 2PMePh₂]⁺). Anal. calcd for C₅₈H₄₂N₈P₂Ru·1.5CH₂Cl₂: C, 62.61; H, 3.97; N, 9.82. Found: C, 62.73; H, 4.05; N, 9.95.

[Ru^{II}(Pc)(P(Buⁿ)Ph₂)₂] (10b). Yield: 50%. ¹H NMR (300 MHz, CDCl₃): δ Pc 8.99 (m, 8H), 7.84 (m, 8H); H_p 6.70 (m, 4H); H_m 6.28 (m, 8H); H_o 4.40 (m, 8H); Buⁿ 0.07 (m, 4H), -0.14 (m, 6H), -1.34 (m, 4H), -1.85 (m, 4H). ³¹P{¹H} NMR (162 MHz, CDCl₃): δ 9.3. UV-vis (9.3 × 10⁻⁵ M, CH₂Cl₂): λ_{max} (log ε) 302 (4.5), 421 (3.7) sh, 580 (4.2) sh, 639 (4.5) nm. FAB MS: *m/z* 1098 (M⁺), 856 ([M - P(Buⁿ)Ph₂]⁺), 614 ([M - 2P(Buⁿ)Ph₂]⁺). Anal. calcd for C₆₄H₅₄N₈P₂Ru·1.5CH₂Cl₂: C, 64.19; H, 4.69; N, 9.14. Found: C, 64.23; H, 4.78; N, 9.02.

[Ru^{II}(Pc)(PBnPh₂)₂] (10c). Yield: 62%. ¹H NMR (400 MHz, CDCl₃): δ Pc 9.03 (m, 8H), 7.87 (m, 8H); H_p 6.67 (m, 4H); H_m, H'_p 6.21 (m, 10H); H'_m 6.00 (m, 4H); H'_o 4.82 (m, 4H); H_o 4.37 (m, 8H); Bn CH₂ -0.59 (s, 4H). (H'_p, H'_m, and H'_o are the phenyl signals of a Bn group). ³¹P{¹H} NMR (162 MHz, CDCl₃): δ 16.2. UV-vis (4.5 × 10⁻⁵ M, CH₂Cl₂): λ_{max} (log ε) 299 (4.5), 421 (3.4), 581 (3.9), 640 (4.4) nm. FAB MS: *m/z* 1166 (M⁺), 890 ([M - PBnPh₂]⁺), 614 ([M - 2PBnPh₂]⁺). Anal. calcd for C₇₀H₅₀N₈P₂Ru·CH₂Cl₂: C, 68.16; H, 4.19; N, 8.96. Found: C, 68.47; H, 4.19; N, 9.02.

[Ru^{II}(Pc)(P(CH₂CH=CH₂)Ph₂)₂] (10d). Yield: 60%. ¹H NMR (300 MHz, CDCl₃): δ Pc 9.01 (m, 8H), 7.87 (m, 8H); H_p 6.70 (m, 4H); H_m 6.27 (m, 8H); H_o 4.42 (m, 8H); H_b, H_c, H_d 3.61 (m, 2H), 3.23 (m, 4H); H_a -1.09 (d, *J* = 5.31 Hz, 4H). ³¹P{¹H} NMR (162 MHz, CDCl₃): δ 12.2. UV-vis (1.2 × 10⁻⁵ M, CH₂Cl₂): λ_{max} (log ε) 296 (4.5), 420 (3.5) sh, 580 (3.9) sh, 639 (4.3) nm. FAB MS: *m/z* 1066 (M⁺), 840 ([M - P(CH₂CH=CH₂)Ph₂]⁺), 614 ([M - 2P(CH₂CH=CH₂)Ph₂]⁺). Anal. calcd for C₆₂H₄₆N₈P₂Ru·CH₂Cl₂: C, 65.74; H, 4.20; N, 9.74. Found: C, 65.69; H, 4.05; N, 9.88.

[Ru^{II}(Pc)(P(CH₂C≡CMe)Ph₂)₂] (10e). Yield: 58%. ¹H NMR (300 MHz, CDCl₃): δ Pc 9.00 (m, 8H), 7.85 (m, 8H); H_p 6.70 (m, 4H); H_m 6.28 (m, 8H); H_o 4.42 (m, 8H); Me 0.60 (s, 6H); H_a -1.00 (s, 4H). ³¹P{¹H} NMR (162 MHz, CDCl₃): δ 14.4. UV-vis (3.4 × 10⁻⁵ M, CH₂Cl₂): λ_{max} (log ε) 296 (4.6), 420 (3.5) sh, 581 (4.0) sh, 640 (4.5) nm. FAB MS: *m/z* 1090 (M⁺), 852 ([M - P(CH₂C≡CMe)Ph₂]⁺), 614 ([M - 2P(CH₂C≡CMe)Ph₂]⁺). Anal. calcd for C₆₄H₄₆N₈P₂Ru·1.5CH₂Cl₂: C, 64.62; H, 4.06; N, 9.20. Found: C, 64.86; H, 4.03; N, 9.33.

[Ru^{II}(Pc)(P(CH=C=CH₂)Ph₂)₂] (10f). Yield: 44%. ¹H NMR (400 MHz, CDCl₃): δ Pc 9.00 (m, 8H), 7.83 (m, 8H); H_p 6.63 (m,

4H); H_m 6.27 (m, 8H); H_o 4.65 (m, 8H); H_a, H_b 1.27 (m, 6H). ³¹P{¹H} NMR (162 MHz, CDCl₃): δ -0.8. UV-vis (1.4 × 10⁻⁵ M, CH₂Cl₂): λ_{max} (log ε) 299 (4.6), 415 (3.7) sh, 578 (4.0) sh, 642 (4.5) nm. FAB MS: *m/z* 1062 (M⁺), 838 ([M - P(CH=C=CH₂)Ph₂]⁺), 614 ([M - 2P(CH=C=CH₂)Ph₂]⁺). Anal. calcd for C₆₂H₄₂N₈P₂Ru·CH₂Cl₂: C, 65.97; H, 3.87; N, 9.77. Found: C, 66.29; H, 3.72; N, 10.05.

X-Ray Crystal Structure Determinations of 1a, 2b·2CH₂Cl₂, 3b,c, 4, and 5b·2CH₂Cl₂. Diffraction-quality crystals were obtained by the slow evaporation of dichloromethane/hexane solutions at room temperature under argon for **1a** (0.35 × 0.3 × 0.25 mm³) and **2b**·2CH₂Cl₂ (0.5 × 0.3 × 0.25 mm³), by the same method, except that the solution was open to air, for **5b**·2CH₂Cl₂ (0.3 × 0.3 × 0.25 mm³), and by layering pentane on the top of chloroform solutions for **3b** (0.6 × 0.4 × 0.15 mm³), **3c** (0.6 × 0.25 × 0.15 mm³), and **4** (0.4 × 0.3 × 0.25 mm³). Each crystal was mounted in a glass capillary. The data were collected at 28 °C using graphite monochromatized Mo Kα radiation (λ = 0.71073 Å) on a MAR diffractometer with a 300 mm image plate detector (oscillation step of φ, 1.5° for **3b,c** and 2° for **1a**, **4**, **5b**·2CH₂Cl₂; exposure time, 5 min for **4** and 10 min for **1a**, **3b,c**, **5b**·2CH₂Cl₂; scanner distance, 120 mm; images collected, 90 for **5b**·2CH₂Cl₂, 100 for **1a** and **4**, 130 for **3b,c**; the images were interpreted and the intensities were integrated using program DENZO²⁴), except for **2b**·2CH₂Cl₂, the data of which were collected on a Bruker Smart CCD 1000 diffractometer. The structures were solved by direct methods using the SIR-97 program²⁵ (**1a**, **2b**·2CH₂Cl₂, **3b,c**, and **5b**·2CH₂Cl₂) or SHELXS-97 program²⁶ (**4**) on a PC. Many non-H atoms (including P and Fe or Ru) were located according to direct methods and the successive least-squares Fourier cycles. Positions of other non-hydrogen atoms were found after successful refinement by full-matrix least-squares using the SHELXL-97 program²⁷ on a PC. There is half of a formula unit in the asymmetric unit for **1a**, **2b**·2CH₂Cl₂, **3b**, and **5b**·2CH₂Cl₂, whereas the asymmetric unit for **3c** and **4** contains a half of each of the two independent molecules. The H atoms on P in **1a** and **4** were added according to the difference Fourier map and refined isotropically; those in **3c** were added with idealized PH₂ geometry, and the P-H bond lengths were restrained to be ~1.45(2) Å. In the final stage of least-squares refinement, all non-hydrogen atoms were refined anisotropically. H atoms on C atoms were generated by the program SHELXL-97. The positions of these H atoms were calculated on the basis of the riding mode with thermal parameters equal to 1.2 times that of the associated C atoms and participated in the calculation of final *R* indices.

Acknowledgment. This work was supported by The University of Hong Kong (Seed Funding for Basic Research), Hong Kong Research Grants Council (HKU7026/04P), and the University Grants Committee of the Hong Kong SAR of China (Area of Excellence Scheme, AoE/P-10/01).

Supporting Information Available: Figure S1 and positional and thermal parameters and bond lengths and angles for **1a**, **2b**·2CH₂Cl₂, **3b,c**, **4**, and **5b**·2CH₂Cl₂ in CIF format. This material is available free of charge via the Internet at <http://pubs.acs.org>.

IC800484K

(26) Program for the Solution of Crystal Structures: Sheldrick, G. M. *SHELXS-97*; University of Göttingen: Göttingen, Germany, 1997.

(27) Program for the Refinement of Crystal Structures: Sheldrick, G. M. *SHELXL-97*; University of Göttingen: Göttingen, Germany, 1997.